Meteorol. Z. (Contrib. Atm. Sci.), PrePub DOI 10.1127/metz/2022/1106

PrePub Article

The Karlsruhe temperature time series since 1779

Michael Kunz[1*], Christoph Kottmeier[1], Wolfgang Lähne[2], Ingo Bertram[3] and Christian Ehmann[4]

[1]Institute of Meteorology and Climate Research (IMK), Karlsruhe Institute of Technology (KIT), Karlsruhe, Germany
[2]POLLICHIA Verein für Naturforschung und Landespflege e.V., Neustadt an der Weinstraße, Germany
[3]hr, ARD-Wetterkompetenzzentrum, Frankfurt, Germany
[4]Deutscher Wetterdienst DWD, Munich, Germany

(Manuscript received August 3, 2021; in revised form December 10, 2021; accepted January 24, 2022)

Abstract

This paper presents the long-term Karlsruhe temperature series re-digitized and reconstructed from handwritten manuscripts from 1779 to 1875 archived in various libraries. Despite great efforts, data from some periods remained missing in the manuscript departments so that the main Karlsruhe series remained partially fragmented. Combined with historic climate records available in the archive of German Weather Service (DWD), the entire series until 2008, when the official Karlsruhe station was relocated to Rheinstetten, is one of the longest climate series available for Germany. The series includes various observational parameters on a daily or even sub-daily basis converted into SI units or contemporary units.

The focus of this paper is on the temperature series and presents some first statistical analyses to demonstrate the additional benefit of possessing unique long-term instrumental climate data on a sub-daily basis. The entire temperature series was homogenized with respect to consistent observation times and to an urban boundary site. It is shown that the width of the distribution function quantified from constructed daily maximum and minimum temperature has substantially broadened in the summer months, but not during winter or the entire year. The number of summer and hot days has substantially increased in the last 30–50 years, while the number of frost and ice days has decreased. Summer or hot days as well as heat waves were very rare before 1920, being unrepresentative of a period mainly unaffected by climate change. Singularities of the climate system, such as the (cold) Schafskälte in June or the (warm) Hundstage in July/August, are clearly shown in most periods. The (cold) Ice Saints in May, however, have a high frequency only in the coldest period between 1870 and 1960; they are hardly detectable in most of the preceding years. Temperature statistics show that the severity of late spring frosts has gradually increased during the entire record mainly as a result of later frost occurrences.

Keywords: long-term climate series, digitization, homogenization, temperature variability, temperature trend, statistics

1 Introduction

Long-term instrumental observations of meteorological parameters are of paramount importance for a better understanding of natural climate variability, for investigating historical extreme events, and for validating climate model simulations on various time-scales. Daily surface pressure data, for example, are needed to create a daily historical European–North Atlantic mean sea level pressure dataset (EMSLP; Ansell et al., 2006) or to reconstruct historical atmospheric circulation patterns in the Twentieth Century Reanalysis project (20CR, Compo et al., 2011). Long-term homogeneous pressure and temperature records have been used to scrutinize single years with large deviations from the mean seasonal cycle and to relate those years to the historical context, such as the "year without a summer" of 1816 (Brönnimann, 2015, Brugnara et al., 2015) and the 2003 European heat wave (Trigo et al., 2005).

In Germany, records of climate observations over a period of more than 200 years are only available for a few sites. A series of daily temperature observations since 1701 is available for the city of Berlin, being the longest existing series. However, as noted by Cubasch and Kadow (2011), during the first 150 years, measurements were problematic because locations, instruments and measurements changed frequently and without proper documentation. The Societas Meteorologica Palatina, established in 1781 to coordinate observations of the weather on an international scale (Aspaas and Hansen, 2012), started with meteorological measurements, including phenomenological observations in Mannheim already in 1781 (state of Baden-Württemberg, SW Germany; Schnelle, 1955). The series, however, is not completely preserved. Other long-term records are available for Regensburg (Bavaria,

*Corresponding author: Michael Kunz, Institute of Meteorology and Climate Research (IMK), Karlsruhe Institute of Technology (KIT), Karlsruhe, Germany, e-mail: michael.kunz@kit.edu

SE Germany; temperature observations since 1773; Auer et al., 2007), Munich and the mountain station of Hohenpeißenberg (both Bavaria and both since 1781; Winkler, 2009), Bremen (state of Bremen, NW Germany; since 1803; Olbers, 2013), and Stuttgart-Hohenheim (Baden-Württemberg; 1792), where daily observations until 1878 were discarded because of bad installation of the instruments and incompleteness of the data (Wulfmeyer and Henning-Müller, 2006). All climate records involve undocumented or scarcely documented measurement and instrument changes as well as changes in the observation methods and times.

The climate of the Karlsruhe region is exceptionally warm and moist, particularly due to its location in the broad Upper Rhine valley north of the Burgundy Gate, through which Mediterranean air masses are frequently advected (Höschele and Kalb, 1988; REKLIP, 1995). Mean temperature (1980–2010) at Karlsruhe is 11.03 °C (DWD, 2021a), being the 5th warmest of all 265 DWD synoptic stations (8.81 ± 1.56 °C). Besides, the temperatures often reach the highest values in all of Germany; until 2018, Karlsruhe held the temperature record of 40.2 °C (2003) together with two other stations in Germany. Because of these extraordinary climatic characteristics and the founding of the first meteorological association, the Societas Meteorologica Palatina, in the neighboring city of Mannheim in 1781, high-quality meteorological measurements and regular observations have been performed in Karlsruhe since 1776. In addition to the observation series of Berlin, Mannheim and Hohenpeißenberg, the Karlsruhe series is thus one of the longest and is unique because of its multitude of available parameters, such as wind speed and direction, precipitation, cloud cover, and significant weather reports (fog, thunderstorms, graupel, hail among others).

In the archives of the German Meteorological Service (*Deutscher Wetterdienst*, DWD), a quality assured long-term climate series for Karlsruhe with three observations per day at the so-called Mannheim hours (*Mannheimer Stunden*; 7, 14 and 21 local time, LT) is available for the period from 1 January 1876 to 31 October 2008 (DWD, 2020). Comprehensive meteorological observations, however, were already performed by Johann Lorenz Böckmann on a regular basis beginning in 1776, later continued by his son, Carl Wilhelm Böckmann, and others (see Table A1). Temperature observations since 1779 are available in historical data archives, such as the Global Historical Climatology Network (GHCN; Menne et al., 2018) and the Historical Instrumental Climatological Surface Time Series of the Greater Alpine Region (HISTALP; Auer et al., 2007). However, only monthly mean temperatures are available (even though GHCN stated on their homepage that mean monthly maximum and minimum temperatures as well as monthly total precipitation will be included at a later date).

Handwritten records of daily and even sub-daily climate observations since the end of the 18th century are archived in the handwritten manuscript departments of the university libraries of Karlsruhe and Heidelberg, the municipal archive of Mannheim, the DWD library and, as excerpts, from three Karlsruhe local newspapers. The records include several meteorological variables, such as temperature, pressure, relative humidity, wind speed and direction, precipitation and hail, cloud cover, and significant weather reports.

With great effort, we have digitized and reconstructed the entire Karlsruhe climate series, including partial series from other observers, for the years from 1779 to 1875. Despite countless searches and trawling through various archives in relevant libraries, the series however remained fragmented before 1800.

Because of the high relevance for climate change as well as to demonstrate the additional benefit of possessing unique long-term instrumental climate data on a sub-daily basis for better understanding the climate variability in an era unaffected by anthropogenic climate change, this study presents some first statistical analyses of temperature observations solely. The newly digitized temperature series before 1876 was homogenized in a pragmatic way with respect to consistent observation times and referring to an urban boundary site. Furthermore, maximum and minimum temperatures were constructed by applying a mean characteristic daily temperature cycle for 10-day periods. Finally, the series was combined with data from the archive of DWD until 2008, when the observation site in Karlsruhe was terminated. All subsequent analyses are based on the homogenized and merged temperature series, referred to as "Karlsruhe temperature series" hereinafter; the term "Karlsruhe climate series" refers to the entire observations.

The paper is structured as follows: Section 2 briefly describes how we collected and digitized the handwritten manuscripts of the Karlsruhe observations, while Section 3 introduces the Karlsruhe temperature series including their homogenization and reconstruction of daily minimum and maximum temperature. Section 4 briefly discusses monthly means of the newly digitized temperature series and shows the deviations from the GHCN series. The main part, Section 5, investigates long-term variabilities and gradual changes in the temperature distribution, seasonal cycle, and different temperature indices with a focus on the period before 1876, for which we have newly digitized the data. Attention is also paid to singularities, such as the well-known "Ice Saints" in mid-May, and to late frost occurrences. This section closes with a brief discussion of the potential benefit of possessing daily temperature records for better understanding the adverse weather conditions associated with the well-known, popularly so-called "year without a summer", 1816.

2 The newly digitized Karlsruhe climate series 1779–1875

The Karlsruhe climate series is a compilation of various meteorological observations recorded in the city

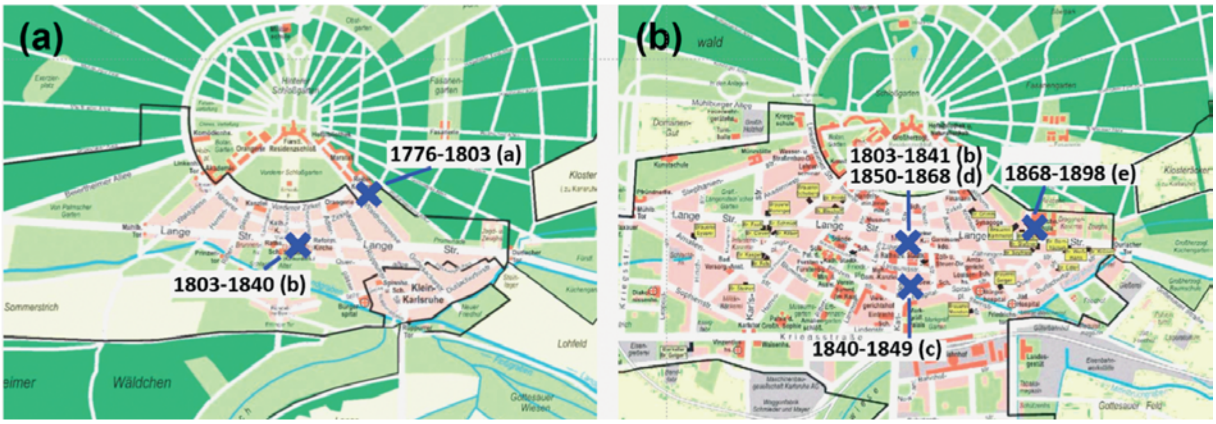

Figure 1: Meteorological observation sites on maps of the town in 1790 (a) and 1868 (d). Source of maps: http://www.maegges.net/karlsruhe/.

of Karlsruhe dating back to 1779 (fragmented even to April 1778). As with any long-term series, the Karlsruhe climate series includes observations made by different institutions and operators based on different standards and instruments and recorded at different locations. The entire series consists of two main parts: the newly digitized climate series from 1779 to 1875 and the data from the DWD archive (WMO code 10727) between 1876 and 2008. During the entire 231-year period, the Karlsruhe station was relocated nine times (see Table A1 in the Appendix), but most of the time it was located on the boundary or periphery of Karlsruhe.

The following sections introduce the newly digitized climate series, including the station locations and instrumentations, present a simplified data homogenization approach for the temperature records to considering changes in observation time and station location, and show the construction of minimum and maximum temperatures (*Tmin* and *Tmax*). Afterward, we briefly describe the compilation of the entire Karlsruhe temperature series, including the filling of short-term data gaps.

2.1 General description and station locations

The entire newly digitized daily Karlsruhe climate series includes several meteorological observations: The temperature at different sites (outside in the street and/or in the courtyard, at barometer level), air pressure, cloud coverage, wind speed and direction, relative humidity, precipitation totals, and reports of significant weather (light/heavy/liquid/solid precipitation, hail, graupel, dew, rime, dust, fog, thunderstorm, and lightning). All observations were converted into SI-units or contemporary units (e.g., °C, hPa, m s^{-1}). The observer usually measured three times a day – usually at the Mannheim hours – but sometimes at different times and with temporary observation gaps (see also Section 3.1a). Additional information about the instruments used, their calibration, and the readout of the data as well as the altitude of the barometer installation are well documented in the literature (see Tables A1 and A2 in the Appendix).

The systematic recording and collection of meteorological measurements in Karlsruhe as the first observation station in southwest Germany are closely linked to the development of the University of Karlsruhe, founded in 1825 under the name Polytechnicum (TH). The first observations between 1776 and 1789 with several gaps were conducted by J.L. Böckmann. After 1798 (available only after 1800), this task was assumed by his son, C.W. Böckmann. What happened in the intervening period is unclear; no records were found in the archives, even though monthly means are available in the archives of GHCN and HISTALP. Until 1803, the meteorological station was located at the village border (*Innerer Zirkel*; location a in Fig. 1a). In 1803, the station moved to the physical cabinet of the Polytechnical Institute in the lyceum building at the Karlsruhe marketplace, approximately 400 m to the southwest of the former location, where it acquired some characteristics of a city station (location b in Fig. 1a). Almost the same instruments were used in similar ways inside and outside the home of the director of the lyceum. In 1840, the station was relocated 100 meters to the physical cabinet in the *Spitalstrasse* (location c Fig. 1b). In 1850, the station moved to the Polytechnicum in the lyceum building of the Karlsruhe marketplace, the same location as some years ago (location d, same as b, in Fig. 1b); the exact location, however, remains unknown. Another small relocation, probably within the lyceum building, occurred in 1865. After 1868 (and until 1895), the station was established in the western wing of the Polytechnicum in the *Lange Strasse* (today: *Kaiserstrasse*) near the northern limit of the build area of Karlsruhe, which at that time was only 70 m from the extended forest *Hardtwald* (location e in Fig. 1b). The various relocations may have caused abrupt changes in the time series. By contrast, increasing urbanization, such as at the lyceum location near the marketplace, which became an inner-urban site in the 19th century, can be assumed to result in gradual changes. This issue is addressed below.

In addition to the main series described above, meteorological recordings were temporally performed in parallel by other observers at other locations within

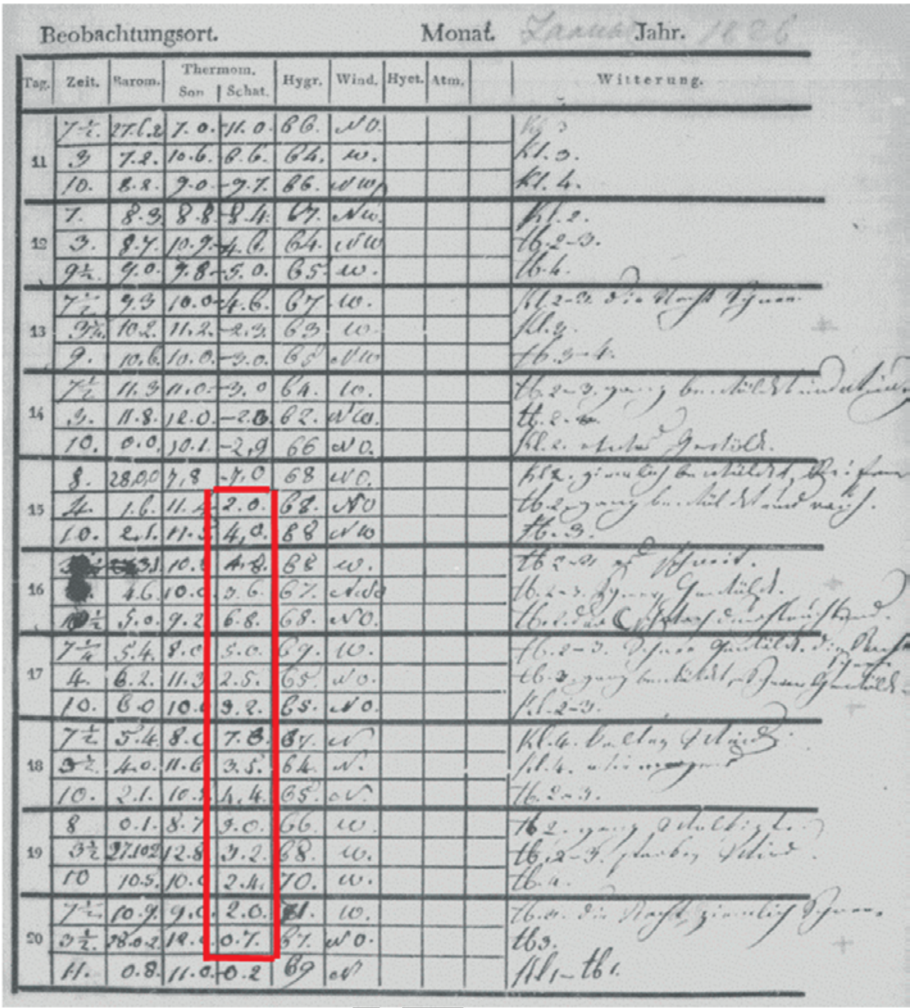

Figure 2: Example of a scanned copy documenting meteorological measurements and observations from 11 to 20 January 1826 with three observations per day (three lines; rows from left to right: day, time, station pressure, temperature I (indoor) and II (outdoor), relative humidity, wind direction, and weather conditions; the red frame is for a comparison with another handwritten copy shown in Figure B1 in the Appendix).

the city. Such parallel series prevail for the periods 1829–1851 (by Eisenlohr), 1850–1860 (by Klauprecht), and 1852–1856 (by Weber). Metadata, such as information about the instrumentation and the calibration, are only available for the latter observer. Despite the lack of metadata, we used the parallel series not only for a systematic comparison with the main series to detect outliers or transcript failures but also to fill some of the data gaps in the main series (cf. Section 3.4).

2.2 Digitization

The Karlsruhe main and parallel climate series are based on high-resolution scans of either original handwritten meteorological diaries and climate tables or handwritten copies thereof. These documents are stored in the manuscript departments of the libraries of the Universities of Karlsruhe and Heidelberg, the city archive of Mannheim, and the paper archive of DWD in Offenbach (see Table A2 in the Appendix). Parts of the time series are supplemented by reports from local newspapers. Between 1801 and 1821, the records of the Karlsruhe manuscripts are summarized copies of the second observer, C.W. Böckmann (see the example in Fig. 2).

All handwritten climate records were manually digitized from the scans with considerable effort. More than one million entries were entered manually using the numeric keypad. Tests with automatic optical character recognition (OCR) turned out to be too error-prone, especially because of the ancient and varying scriptures. Because transfer errors cannot be fully excluded, a plausibility control was performed based on threshold tests of absolute values. Implausible values were again compared with the scans and corrected if necessary. After a second quality check, all observations were converted into metric values and standard units (e.g., °C, mm, hPa). In addition, all temperature observations were manually verified regarding outliers and inconsistencies, such as temperature values that do not fit the season.

During the digitization it turned out that, in some cases, the temperature records archived in the manuscript departments of the Karlsruhe and Heidelberg libraries are not identical. An example is shown in Figure B1 in the Appendix, where the temperature observations between 15 and 20 January 1826 have opposite signs in the manuscripts archived in the libraries of Karlsruhe and Heidelberg. It can be assumed that one of the handwritten manuscripts is a copy of the other, and mistakes were made when transcribing the original manuscript. Because of varying scriptures, it was sometimes not possible to distinguish the copy from the original.

In addition, some of those who worked on the transcripts at that time tried to adjust the temperature values on sunny days to the observation times, which often deviated from the Mannheim hours. For this reason, we digitized all temperature series available in the manuscript departments. Statistical methods that compare two different samples (e.g., Mann-Kendall or Mann-Whitney-U test) are of limited help regarding the question of which records have already been corrected and which have not. For this decision, we considered also other observations, such as cloud cover or precipitation – in addition to the considerable experience we gained during the digitization.

3 The Karlsruhe temperature series

3.1 Homogenization of the temperature series 1779–1875

Homogenization of any observational data is a challenging task mainly because the data are subject to several influencing factors that can cause either abrupt or gradual changes in the time series. Potential influencing factors may result from the instrumentation and their reliability, the observation times, the surroundings, and the station itself regarding the cabin or building structure. A prerequisite of any homogenization is sufficient documentation of the station history, which is the case for the Karlsruhe climate series. Although the application of standard homogenization approaches in general provides satisfactory results for monthly temperature records (Böhm, 2006), a closer examination of the Karlsruhe series homogenized in different projects (HISTALP, Auer et al., 2007; GHCN-V4, Menne et al., 2018; DWD-Archive via ftp) shows considerable discrepancies (not shown here).

The homogenization of monthly values leads to considerable differences, and even greater uncertainties are expected when homogenizing observations on a daily or sub-daily basis. Thus, we applied a simplified, two-step correction method to the temperature series 1779–1875 with a correction for changes in observation times until 1842 and a simplified homogenization with respect to the station location. The changes in the instrumentation in 1840 (see Table A1) did not have a detectable influence on the time series and, thus, was not considered. Due to the lack of detailed information, influencing factors and disturbing effects, such as the aging of the thermometer glass, could not be considered. Other climatic variables, such as wind or humidity, have not yet been homogenized because the implementation is much more difficult compared to that of the temperature.

(a) Homogenization of the temperature series with respect to observation times

Since the 19th century, meteorological observations in Germany and worldwide have usually been collected the so-called Mannheim hours (7, 14, 21 LT,). The observations in Karlsruhe were also taken three times a day before 1843, but at varying times, often one or two hours before or after the Mannheim hours, and sometimes with changes from day to day. The morning observations shown in Fig. 2, for example, were taken at 7:00, 7:30 or 8:00 LT, while afternoon observations were at 15:30 or 16:00, and evening observations at 20:30 or 21:00 LT. Most of the parallel series have this problem as well.

The conversion of the temperature observations to the Mannheim hours is based on the shape of the diurnal temperature distribution estimated from hourly observations at the Karlsruhe DWD station between 1976 and 2008 (reference period). The method we have developed and extensively evaluated is described below; it relies on the characteristic diurnal temperature cycle during the reference period. One must be aware that the temperature correction does not work reliably if the air mass and/or its characteristics changed within a short period of time, for example, as a result of a frontal passage or the cold air outflow of a thunderstorm. This source of error can hardly be eliminated but is not considered to be a severe problem in view of the objective of investigating the temperature variability in the period prior to the beginning of official climate recordings in 1876.

In the first step, hourly temperature means are determined for the reference period by considering prevailing weather conditions, mainly cloud cover, and the time of the year. Because of the considerable variability of the diurnal temperature cycle in the course of a year, the hourly means are further subdivided into 10-day means (hereinafter referred as decade), resulting in a 24×36 matrix: $\overline{T_h^d}$ ($h = 24$ indicates the hour, $d = 36$ the decade). Next, an artificial diurnal temperature cycle T'_h is reconstructed for each day in the period 1779–1875 by adjusting $\overline{T_h^d}$ for the reference period to the three observations T_j^* at different times (j =1*, 2*, and 3* at morning, noon, and evening) for the corresponding decade d. In this step, the diurnal series is separated into three time periods, which are treated slightly differently.

(1) Between the first observation T_1^* in the morning and the second observation T_2^* around noon, hourly values T'_{h1} are calculated using the following approach:

$$T'_{h1} = T^*_{1*} + k_1 \left(\overline{T_h^d} - \overline{T_{1*}^d} \right) \quad \text{with} \quad k_1 = \frac{T^*_{2*} - T^*_{1*}}{\overline{T_{2*}^d} - \overline{T_{1*}^d}}; \tag{3.1}$$

the subscripts 1* and 2* correspond to the observation times j of the new series and not to the hour of the day. The temperature T'_{h1} thus is obtained from the first observation of the day plus an expected temperature change until the searched time $h1$ according to the diurnal cycle of the long-term reference period, multiplied by a correction factor. The latter factor k_1 adjusts the temperature amplitude on a given day and allows for a deviation from the reference diurnal cycle as a result of, for example, cloudiness or cold air advection. This factor is well defined when the denominator is large, meaning that the long-term mean temperatures in the morning and at noon, $\overline{T^d_{1*}}$ and $\overline{T^d_{2*}}$, differ significantly from one another, which is mainly the case during summer time. If the recorded observation time is between whole hours, it is linearly interpolated between the whole-hour means (this applies also to the transformations (2)–(4) below).

(2) A similar approach is applied for the hours between noon and evening:

$$T'_{h2} = T^*_{2*} + k_2\left(\overline{T^d_h} - \overline{T^d_{3*}}\right) \quad \text{with} \quad k_2 = \frac{T^*_{3*} - T^*_{2*}}{\overline{T^d_{3*}} - \overline{T^d_{2*}}}. \tag{3.2}$$

(3a) Between the evening and the following morning, the procedure must be modified. The temperatures at the two times 3* (evening) and 1* (morning) are frequently similar with the consequence that the denominator of the correction factor is very small and the method fails. Therefore, k_3 is calculated as the mean of the well determined factors k_2 of the current day (evening) and k_{1f} of the following day (morning), in total:

$$T'_{h3} = T^*_{3*} + k_3\left(\overline{T^d_h} - \overline{T^d_{3*}}\right) \quad \text{with} \quad k_3 = \frac{1}{2}(k_2 + k_{1f}). \tag{3.3}$$

(3b) The estimate of k_3, however, requires an additional correction. The evening temperature quantified using Eq. (3.3) usually matches the observed values very well. Because k_3 is not calculated directly from temperature observations at the evening and subsequent morning, but instead from the factors k_2 and k_{1f}, the reconstructed temperature curve does not necessarily match the early observation well. Thus, the temperature values of the morning hours are corrected using a linear form:

$$\tilde{T} = T^*_{1f*} - T^*_{2*} - k\left(\overline{T^d_{1f*}} - \overline{T^d_{2*}}\right) \tag{3.4}$$

$$T'_{h3;\mathrm{cor}} = T'_{h3} + \tilde{T}(t'_{h2} - t)/(t'_{h2} - t'_{h1}) \tag{3.5}$$

with t as time. Note that in the above equation the index "*1*" always refers to the following day, thus denoted to as "*1f*". The temperatures at night, T'_{h4}, comprise a part of the long-term mean plus a deviation that is added linearly. The latter component is large if the temperature has changed in an untypical way during the night, for example, as a result of an air mass exchange.

Based on Eqs. (3.1) to (3.4), the temperature observations were converted to every whole hour, including the required Mannheim hours. Daily mean temperatures (*Tmean*), finally, were calculated according to the following formula using the values adjusted to the Mannheim hours (subscripts in Eq. (3.6)):

$$Tmean = \frac{1}{4}\left(T'_{07} + T'_{14} + 2T'_{21}\right), \tag{3.6}$$

This method with the double weighting of the observation at 21 LT was suggested by Kämtz (1831) to provide the best estimate of the daily mean for this combination of observation times. It was the standard method for the daily mean calculation at DWD until 31 March 2001; since April 2001, daily means have been calculated from all hourly observations (Kaspar et al., 2016).

Despite the somewhat artificial character of the temperature adjustment described above, the differences between the uncorrected and corrected data are rather small. The 10-day means of the time-corrected Karlsruhe main series, for example, differ from the uncorrected values for 10-day-averages by only 0 to +0.1 K in the winter, and by +0.1 to +0.5 K in the summer.

(b) Homogenization with respect to station relocations

As discussed above, the observations of the Karlsruhe climate series were conducted at different locations in the city of Karlsruhe, which may cause some abrupt discontinuities (even though such changes cannot be detected in the monthly means shown in Fig. 4). In addition, the increasing expansion of the city caused some locations to become more characteristic of inner-urban sites over time. Various approaches have been employed to detect inhomogeneities and adjust climatic series to compensate for associated biases (e.g., Peterson et al., 1998; Mestre et al., 2011). These methods correct monthly or daily observations, but usually require parallel or neighboring reference series for a similar regional climatic environment (Menne and Williams, 2009).

Because of the sub-daily observations and several available parallel series (urban and suburban), we applied a weather-oriented procedure, where each of the well-documented station changes is declared as a potential break of the series. Based on the above described correction of the inconsistent observation times as well as the correction of the window screens at that time, individual differences of the observations between the parallel series were determined on a decadal basis and in dependence of both the actual weather situation (in particular degree of cover) as well as the season for the period 1779–1875. The difference values obtained in that way form the correction factors of the day-, season-, and weather-specific urban climate effect. Because homogenizing to a location in the center is unreasonable due to the dynamic growth of the city, we homogenized the data with respect to a periphery location. No corrections were applied before 1803, when the observation sites were in urban boundary environments.

Table 1: Monthly factors used to correct the temperature series observed in Karlsruhe between 1779 and 1868 due to changes in the station characteristics. The correction factors are subtracted from the original (and time-corrected) temperature series.

	1779–1802	1803–1810	1811–1820	1821–1830	1831–1840	1841–1850	1851–1860	1861–1868
Jan	0.0	0.6	0.6	0.7	0.8	0.6	0.8	0.8
Feb	0.0	0.6	0.6	0.7	0.7	0.6	0.7	0.7
March	0.0	0.4	0.5	0.5	0.6	0.5	0.6	0.6
April	0.0	0.3	0.3	0.3	0.4	0.3	0.4	0.5
May	0.0	0.2	0.3	0.3	0.3	0.3	0.4	0.4
June	0.0	0.2	0.3	0.3	0.3	0.3	0.3	0.4
July	0.0	0.3	0.3	0.3	0.4	0.3	0.4	0.4
Aug	0.0	0.3	0.3	0.4	0.5	0.3	0.5	0.5
Sept	0.0	0.4	0.4	0.6	0.7	0.4	0.7	0.7
Oct	0.0	0.5	0.6	0.6	0.6	0.6	0.7	0.7
Nov	0.0	0.5	0.6	0.6	0.6	0.6	0.6	0.7
Dec	0.0	0.5	0.6	0.6	0.6	0.6	0.7	0.7
Year	0.0	0.40	0.45	0.49	0.54	0.45	0.57	0.59

Systematic temperature changes in addition were estimated by comparing the main Karlsruhe series with the nearby Mannheim series, which was taken at different locations, partly in urban surroundings and partly near the margin of the build area. The periods considered for the temperature adjustment were as follows: 1776–1792 and 1860–1871 (western wing of Mannheim castle), 1821–1827 and 1853–1857 (observatory, outskirts); 1841–1852 and 1857–1860 (inner city, square C3,18), 1871–1888 (inner city, square N3,4), and 1888–1943 (Mühlausschleuse harbor, outskirts of Mannheim). Because the location changes occurred in different years in Karlsruhe and Mannheim, the periods with only one or both stations in urban environments were inspected to detect, and roughly correct for, urban climate effects. During that period, the slightly higher temperatures in Mannheim (by approx. 0.4 K on average) can be attributed to the early morning exposure of the thermometer to sunshine.

We performed a temperature correction on a monthly basis using constant values for different time periods. The additive correction factors displayed in Table 1 vary between approximately 0.3 K in summer and 0.7 K in winter. Even though obvious errors and implausible values have been eliminated as much as possible, there remains some uncertainty in the data, which may result from transmission errors, errors in the transcripts, or the time adjustment.

After the homogenization of the data as described above, we performed thorough verification regarding outliers and inconsistencies, such as temperature values that do not fit the season. Potential outliers and inconsistencies were marked in a first step using low-threshold plausibility control algorithms. In a further step, the marked data were visually checked against the preceding and following data, the non-homogenized raw data, the weather characteristics on that day and – in some cases – with data sets of the parallel series from Karlsruhe as well as the climate series of Mannheim, Worms, Hanau and Frankfurt, which were also digitized on a sub-daily basis.

3.2 Construction of daily minimum and maximum temperatures 1779–1875

Because the temperatures at the Mannheim hours do not necessarily coincide with minimum and maximum temperatures, *Tmin* and *Tmax*, respectively, these have to be constructed applying an approach different from that described above. The starting point is that the newly digitized temperature observations, in addition to the regular observations, include observed *Tmin* and *Tmax* over a period of almost 13 years (14 Nov 1841 to 28 Aug 1854 with some short-term gaps).

The construction of *Tmin* and *Tmax* starts with the quantification of the temperature differences ΔT between the thrice-daily temperature observations at 7, 14, and 21 LT (Mannheim hours) and the recorded extremes:

$$\Delta T_1^d = \left(T_1^{*d} - T^{d*}min\right), \tag{3.7}$$

$$\Delta T_2^d = \left(T_2^{*d} - T^{d*}max\right), \tag{3.8}$$

Because the diurnal temperature cycle is strongly controlled by incident solar radiation and therefore changes considerably during the year (e.g., *Tmax* in January is reached at 13 UTC, in July at 14 UTC), Eqs. (3.7)–(3.8) are computed separately as means for each of the 36 decades d. In the next step, the temperature differences ΔT_1^d (Eq. (3.7)) are used to construct *Tmin*, whereas ΔT_2^d is used to quantify *Tmax* for periods where no direct observations of *Tmin* and *Tmax* are available. In the evaluation of the temperature differences, it turned out that the temperature observation at night, T_3^{*d}, is not suitable for estimating *Tmax*.

As shown in Fig. 3, the differences ΔT_2^d obtained from Eq. (3.8) to construct *Tmax* are much smaller on average than ΔT_1^d from Eq. (3.7) used to construct *Tmin*. This result means that the second observation (T_2^*) is temporally much closer to *Tmax* than the first observation (T_1^*) is to *Tmin*.

The two differences also show an annual cycle with the largest difference during summer and the smallest

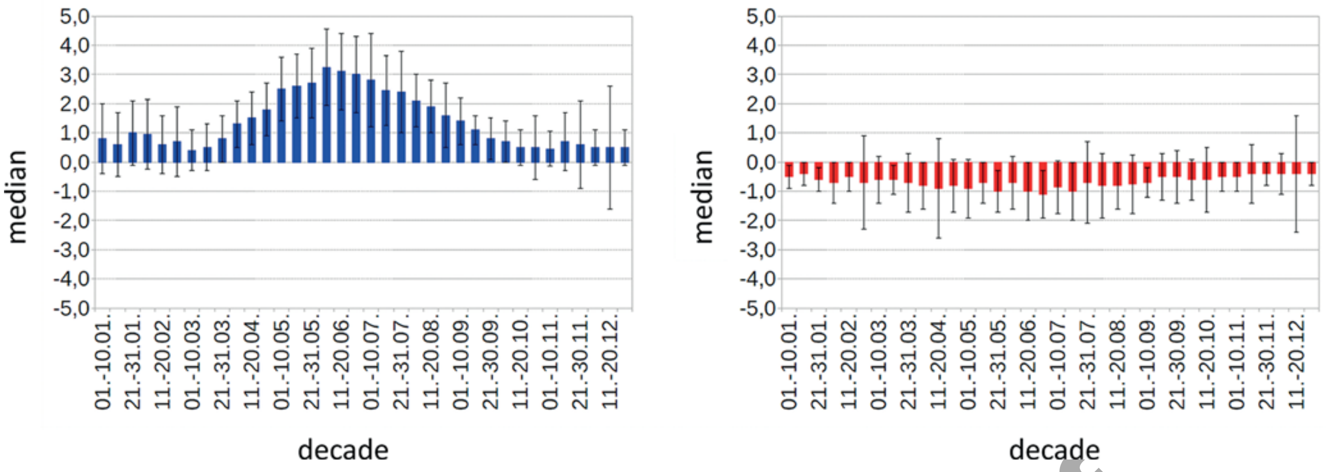

Figure 3: Median and standard deviation of the differences between the morning temperature (7 LT; date value 1) and the lowest temperature (left) as well as the afternoon temperature (14 LT) and the highest temperature (right) during the period 14 Nov 1841 to 28 Aug 1854. The 10-day means are used to construct *Tmin* and *Tmax* for periods with no extreme temperature observations.

in winter resulting from the general diurnal temperature cycle. The values of ΔT_1^d during the winter decades are similar to those of ΔT_2^dduring the summer in a range of 0.5–1 K. This result means that the uncertainty in *Tmin* – most relevant during the winter months – and that in *Tmax* – most relevant during the summer months – are almost identical. This finding is an important issue when calculating temperature indices based on fixed thresholds, such as hot days or ice days (cf. Section 5.3).

Finally, the median values per decade shown in Fig. 3 were added or subtracted to construct *Tmax* and *Tmin* from the observations of T_2^* and T_1^* for the entire period from 1 April 1779 to 31 December 1875. Only in the time frame where *Tmin* and *Tmax* were directly observed did we keep these temperatures. Afterward, we checked the entire series (including the observed *Tmin* and *Tmax* records) for plausibility and for outliers according to the method of Kütting and Sauer (2011). In so doing, we eliminated as many obvious errors and implausible values as possible.

Note again that the temperature extremes *Tmax* and *Tmin* are constructed values and not observed ones (except for the period 1841–1854). The examinations presented in the following sections should therefore be treated with caution regarding the exact values. Nevertheless, they provide a qualitative overview of the weather and temperature conditions and their temporal variability in Karlsruhe during the 18th century.

3.3 The period from 1876 to 2008

Since January 1876, i.e., the end of the newly digitized Karlsruhe climate series, meteorological data for Karlsruhe are available via the DWD data archive. The official synoptic station (SYNOP; WMO code 10727; ID 02522) dates back to that year. Meteorological observations at that time and afterward were much more harmonized, and details can be taken from the literature (Höschele and Kalb, 1988) or from the Open Data server of DWD (DWD, 2021b). For the sake of completeness, we will only briefly describe in the following paragraph the station locations in the city of Karlsruhe.

The Polytechnicum (TH) hosted the meteorological station until 1898, but with two slight relocations within the same building at different heights (location e in Figure B2). Between December 1898 and June 1921, measurements were performed in the University building, just a few hundred meters away. Between 1921 and 1937, the station was operated in the castle *Gottesau*, located approximately 1 kilometer to the east of the previous site and used as a tenement at that time (location g in Figure B2). From April 1937 until October 1944, meteorological observations were recorded on the air base at the outskirts north of Karlsruhe (location h). After an interruption starting from the last months of World War II on 1 November 1944 until September 1945, the operation of the station was resumed in the *Erzberger Strasse*, approximately 1 kilometer south of the former air base (location i). Finally, on 1 November 1977, the station was moved to its final location in the *Hetzstrasse* far off to the northwest outside the city of Karlsruhe, being mainly agricultural land at the periphery of Karlsruhe (location k). Parts of the station, such as the anemometers, were installed at the top of a large building of the "*Landesanstalt für Umwelt* (LUBW)". On 1 November 2008, the DWD station was again relocated to a place near the city of Rheinstetten (WMO code 10731), approximately 7 km south of Karlsruhe. To ensure the continuity of the exceptional long-term Karlsruhe climate series, the IMK has been performing measurements at the same location with the same instruments since 22 January 2009. Extensive vegetation in the immediate vicinity of the station, however, and progressive development in the surrounding area result in too high temperature mainly on high-radiation days in summer. Therefore, we decided not to use this data after 2009.

Even though the data after 1876 are available in the DWD archives, it can be assumed that no thorough homogenization with respect to the different station locations and instruments has been conducted.

3.4 The entire Karlsruhe temperature series

To obtain a most comprehensive and almost complete long-term data record representative for a suburban region, we combined the newly digitized daily temperature series 1779–1875 with observations from the official station later operated by DWD in the period 1876–2008.

Despite great efforts, data from some periods remained missing in the manuscript departments with the consequence that the main Karlsruhe temperature series remained partially fragmented. All major gaps and the series used to fill some of the gaps are listed in Table A3 in the Appendix. Completely missing are the years 1787 and 1788. The largest data gap of the entire series is between 1790 and 1799, where no manuscripts or copies could be found in the archives, even though Pfaff (1810) reported on meteorological observations by J.L. Böckmann at least temporarily in the period 1789–1798. During the 19th century, there were a few shorter gaps lasting between one and 10 days and a longer gap of 116 days from August to November 1851. The short-term gaps were filled with data from the Mannheim series. After testing with temperature values raised or lowered by 2 K during these gaps, the statistics presented later are not sensitive to these changes (except the quantification of threshold days). For the longer gap in 1851, we could use a parallel series in Karlsruhe, which was adjusted to the Polytechnicum site. Note that all these gaps were filled before homogenization and quantification of *Tmin* and *Tmax* (Section 3.1 and 3.2).

The major gap in the DWD time series in 1944/45 could not be filled because no data from adjacent stations were available for this time. The stations of Mannheim und Heidelberg with unbroken series are too far away, and occasionally show large deviations compared to the Karlsruhe site. The last two months in 2008, after DWD terminated their observations at the Karlsruhe station, were supplemented by observations from the DWD station in Rheinstetten. When merging the data, particular attention was paid to days being potential candidates for classification as frost or ice days (see Section 5.3).

3.5 Additional temperature series

For comparative purposes, we also used monthly mean temperature records for the period 1779–1875 from GHCN, which is a set of monthly climate summaries from thousands of weather stations around the world (Vose et al., 1992). We used GHCN version 4, which, in contrast to the previous data, provides a more comprehensive consideration of quality checking and uncertainty for the calculation of station and regional temperature trends (Menne et al., 2018).

4 Monthly mean temperature 1779–1875

We first compare monthly means computed from the newly digitized and homogenized Karlsruhe temperature series with GHCN data (Fig. 4). Note, however, that the purpose of this paper is neither to trace back the differences to their origin nor to investigate temperature variability compared to other regions.

For most years, the temperatures in the Karlsruhe series are slightly higher than those of the GHCN data, yielding a positive bias of $\overline{\Delta T} = 0.19$ K for the period 1779–1875 ($\overline{\Delta T} = -0.01$ K for 1779–1786 before the large gap, and $\overline{\Delta T} = 0.21$ K for 1800–1875). However, the differences between the two series are not constant, showing deviations persisting over several years and abrupt changes. In 55.6 % of all months, the differences are equal to or less than 0.2 K; in 91.2 %, the differences are less than 0.5 K. Larger differences of more than 1 K are rare and occur only 10 times (months). The two series have similar values in the few years of the 18th century, at the beginning of the 19th century until 1825, in the period from 1834 until 1843, and after 1862. By contrast, the largest differences occur between 1853 and 1865. After 1865, two abrupt changes occur with a 3-year time range with negative differences followed by a 6-year time range with almost constant positive deviations. Furthermore, there is a slight tendency for larger deviations during the summer months, which does not apply to the single peak deviations.

The reasons for the deviations are unclear. They are not related to station relocations or instrumental changes. Likewise, they do not result from urbanization, as this would imply gradual changes. We also cannot judge which of the time series is more reliable. Considering other monthly mean temperature series, such as that of the HISTALP database (Auer et al., 2007), the differences with the Karlsruhe temperature series are even smaller. This fact at least suggests that the newly digitized Karlsruhe temperature series is more realistic than GHCN.

The four station relocations, indicated by sr1–sr4 in Fig. 4, have no noticeable effect on the time series – neither on the course of the monthly means nor on the differences. Of course, there are changes in *Tmean*, *Tmin*, and *Tmax* averaged over the partial series between station relocations (colored horizontal bars in Fig. 4). Particularly near the last station relocation in November 1868, temperature means change substantially by approximately 0.4, 1.1, and 1.0 K for *Tmean*, *Tmin*, and *Tmax*, respectively. These changes, however, are within the range of the changes observed between all 20- and 30-year periods of the entire series and are therefore an expression of natural climate variability. Also note that the time span after relocation sr4 is only 8 years; when extending the time span to 20 years, the temperature differences decrease considerably.

The seasonal cycle of most years resembles a normal distribution, which is sometimes very smooth and

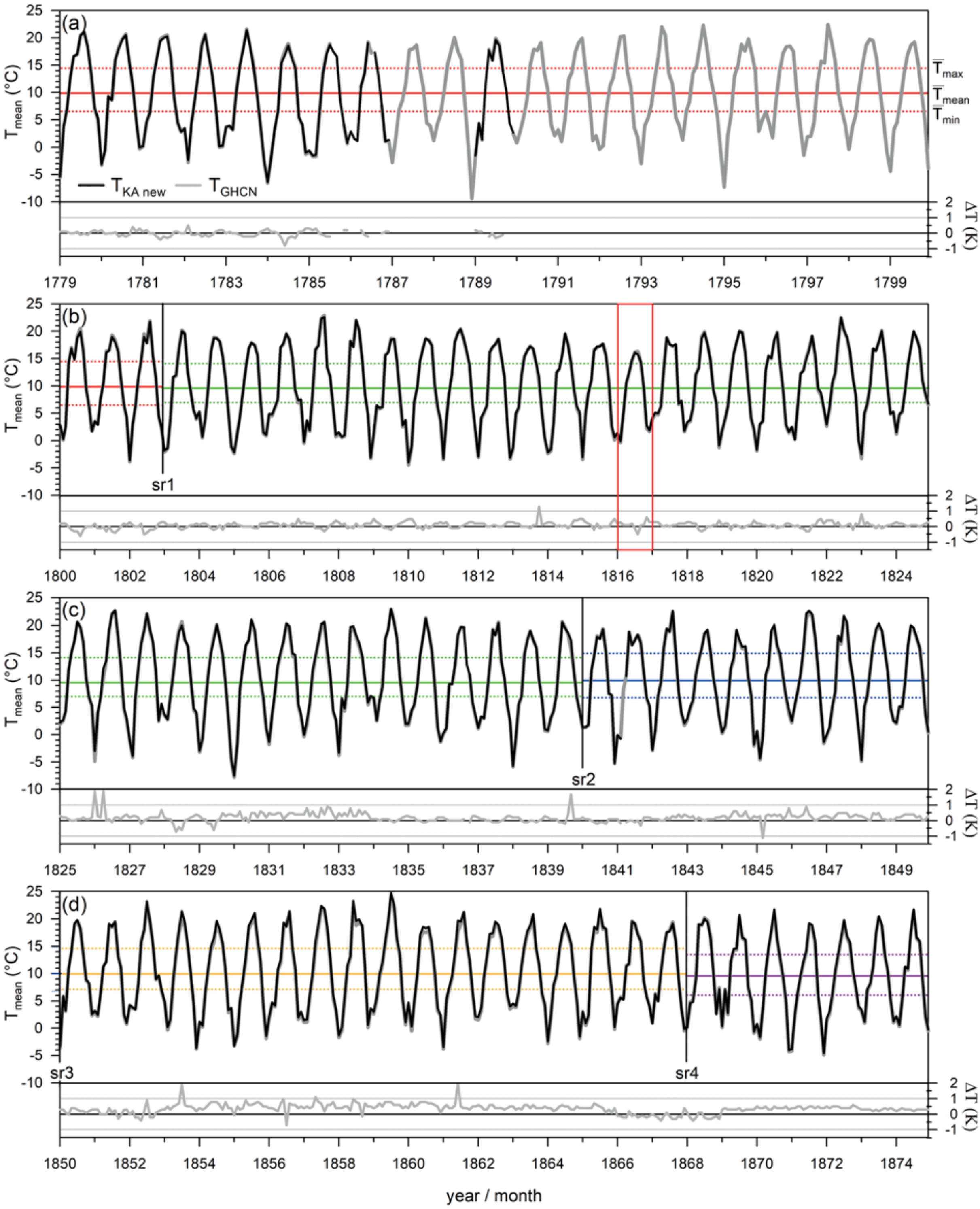

Figure 4: Time series of the monthly mean temperatures of the Karlsruhe temperature series and the GHCN series (upper part of the subfigure s) and the temperature differences between the two series (KA new – GHCN; lower part). Included are *Tmin*, *Tmax*, and *Tmean* of the Karlsruhe temperature series averaged over the time periods between station relocations (indicated by the vertical lines sr1–sr4; cf. Table A1 in the Appendix). *Tmin*, *Tmax*, *Tmean* for the five periods are: 6.5, 14.6, 9.9 °C (1779–1802); 7.0, 14.1, 9.6 °C (1803–1839); 6.8, 14.9, 10.0 °C (1840–1849); 7.1, 14.6, 9.9 °C (1850–1868); and 6.1, 13.5, 9.5 °C (1869–1875). The red box marks the so-called "year without a summer", 1816 (see Section 5.5 and Fig. 13).

sometimes with a slight fluctuation. A few years (e.g., 1789, 1817, 1830, or 1865) show stronger deviations from the general distribution with several upward and/or downward peaks. When inspecting the magnitudes of the monthly means, a large variability in annual and multiannual scales is found. The mean temperature in January, for example, ranges from −7.5 (1830) to 6.8 °C (1834). In the warmest month, July, the variation range is between 16.1 (1816, the so-called "year without a summer") and 24.7 °C (1859).

Compared to other available long-term temperature series, such as De Bilt, Bremen, Berlin, Prague, or Hohenpeissenberg, some similarities, but also discrepancies, can be observed in the annual means (Heinemann, 1994; Winkler, 2009; Olbers, 2013). The slight cooling in the first half of the 19th century (see *Tmean* in Fig. 4 and Figs. 4 and 5 in Olbers, 2013) is also observed in Hohenpeissenberg, Bremen or Prague, while the other stations do not show such behavior (not shown). Interestingly, several anomalies in some years show a surprising agreement, although the stations considered here are quite distant from each other. For example, the negative anomaly in 1829/30 or the positive anomaly four years later in 1834 can be observed at all stations. However, the cooling in the so-called "year without summer" 1816 (see Section 5.5), in which the annual cycle in Karlsruhe is strongly damped, can only be seen in the Hohenpeissenberg series.

5 Temperature variability based on the daily records 1779–2008

The essential advantage of the newly digitized and homogenized Karlsruhe temperature series compared to monthly series, such as the GHCN (Section 4), is the availability of daily observations and constructed extreme temperatures. The daily data allows us to study not only climatic conditions but also temperature variability and changes on the synoptic temporal scale, which is much closer to real weather conditions than any means. Likewise, the assessment of extreme events or periods requires daily data. Extreme events, representing the tail of the distribution function, tend to be more relevant to society than mean values that occur much more frequently (Zhang et al., 2011). Detailed investigations of temperature variability for a period unaffected by climate change helps to better understand the characteristics and strengths of temperature changes associated with natural climate variability. In the following section, we examine temporal changes of different percentiles of the distribution function, seasonal temperature cycles, the temporal variability of various threshold days, and hot/cold spells based on the daily mean, minimum, and maximum temperatures of the entire Karlsruhe temperature series 1789–2008.

5.1 Long-term changes of the distribution function

We start our investigation of past temperature variability at the Karlsruhe station with an analysis of different percentiles quantified from daily mean temperature data for 30-year moving time slices beginning in 1800 because of the very fragmented series before. The percentiles and differences in selected percentiles showing the spread of the distribution function are quantified for the entire year and separately for the winter (Dec.–Feb.) and summer (June–Aug.). Because of the large sample sizes (30 years = 10.957 or 10.958 days), we quantified the percentiles directly from the ordered values without adjusting an appropriate statistical distribution function (a test showed only marginal differences).

For the entire year, the 30-year median of daily mean temperatures (black curve in Fig. 5a) is relatively smooth over almost the whole period of 209 years with values around 10 °C. Besides, it is almost identical to the mean value (difference as red curve in Fig. 5b). Fluctuations on the order of ±0.5 K for the 30-year means are mostly restricted to the 19th century until about 1890. The coldest phase with a mean temperature slightly below 10 °C is from approximately 1817 until 1902, i.e., spanning roughly the time frame 1853–1916 in the 30-year means. Most striking, however, is the strong increase in the 30-year means starting in the 1970s (middle of the 1980s in Fig. 5a) for the medians but up to 10 years earlier for the extreme percentiles. Since the 1970s, the median temperature has increased by almost 0.8 K from 10.4 °C (the 1950s until the 1980s) to 11.2 °C (1979–2008; center 1994).

The general course of all percentiles is more or less similar to the median. However, the closer the percentiles are to the tails of the distribution function, the larger the temporal variability is. The 1st and 99th percentiles (red curves in Fig. 5a), for example, have a fluctuation range of 3.1 and 2.3 K, respectively, which is similar for other extreme percentiles. Interestingly, the coldest phase in the second half of the 19th century coincides with a decrease in the higher percentiles (σ, green; 95th, blue; and 99th, red), but with an increase in the values for the lower percentiles. Particularly the 1st percentile, but also the 5th percentile, shows a gradual increase from 1880 until 1920 (center of the 30-year periods) of 2.5 and 2.2 K, respectively, which means that the cold period was mainly due to a decline in higher temperatures (higher percentiles) and not to an increase in the number of days with lower temperatures (lower percentiles).

The width of the distribution function, estimated using the interquartile and the 2σ ranges, shows the superposition of high-frequency volatility and variations over several decades (Fig. 5b). According to this figure, the distribution function of *Tmean* over 30-year intervals had the widest range near the second half of the 19th century. Afterward, until the 1920s (center of the time series), the distribution again widened. Almost the

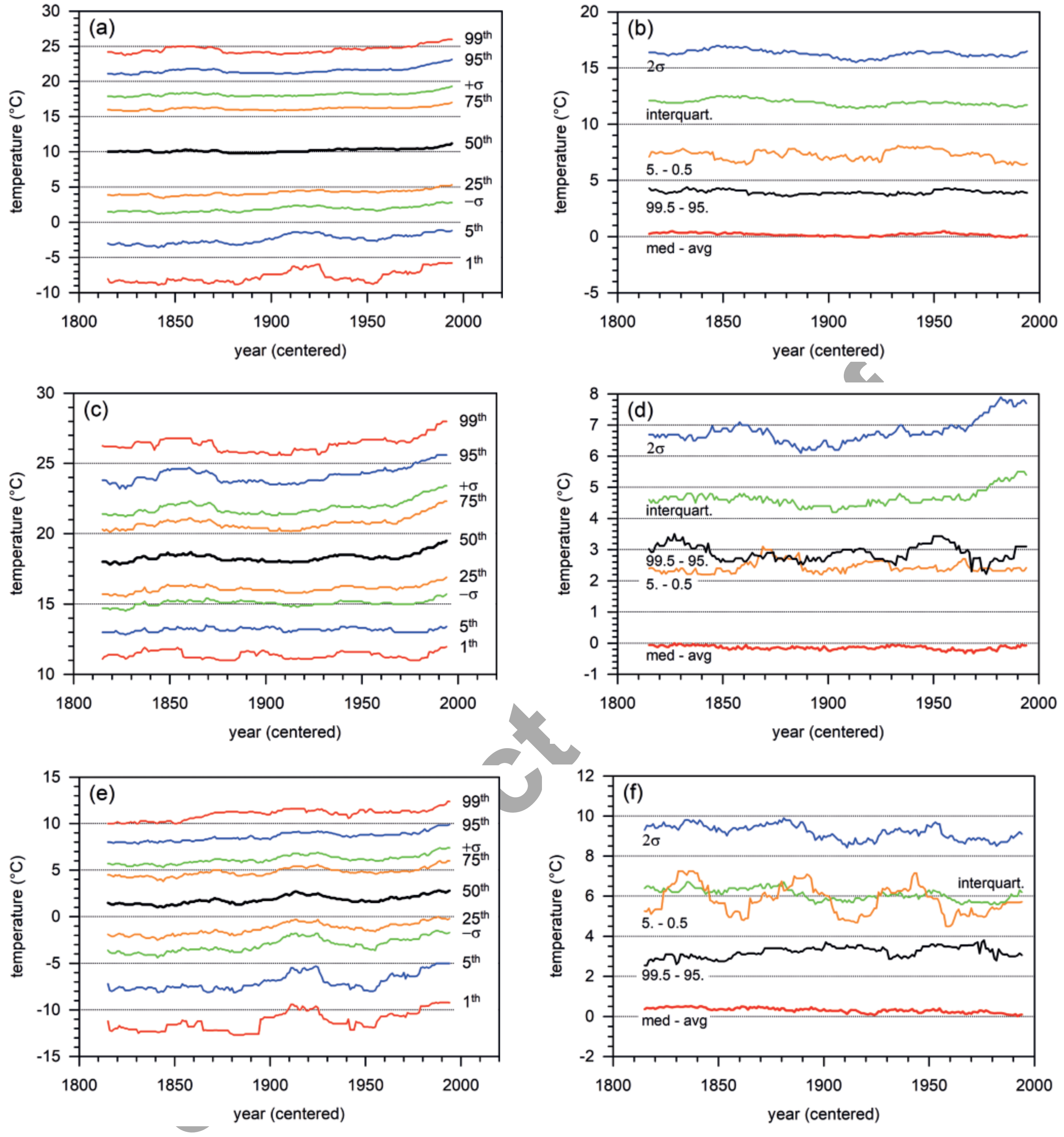

Figure 5: Different percentile values (+σ corresponds to the 84.1th, $-\sigma$ to the 15.9th percentile) of the daily mean temperature of 30-year moving time slices (a+c+e) and the differences in the most important percentiles (2σ, interquartile range, 5th–0.5th and 99.5th–95th percentiles, median–mean) to estimate changes in the spread of the 30-year distributions (b+d+f) for the entire year (a–b), the summer (June–Aug.; c–d), and the winter half-year (Dec.–Feb.; e–f); the x-axis displays the centers of the 30-year periods (e.g., the first value 1815 refers to the 1800–1829).

same long-term variability is found for the difference between the median and mean.

During most years, including those of the newly digitized time range, the median values are larger than the means, indicating that the distribution function is slightly shifted by about 0.5 K to higher temperature values. When looking at the two tails of the distribution function, we see higher values and a larger variability in the lower tail (5th–0.5th perc.) compared to the upper tail (99.5th–95th perc.). This result means that the year-to-year variability of colder days, potentially being frost or ice days, is much higher than those of warm and hot days.

Considering only the summer months, all percentiles show a larger annual and multi-decadal variability, even if the variability of the higher percentiles of

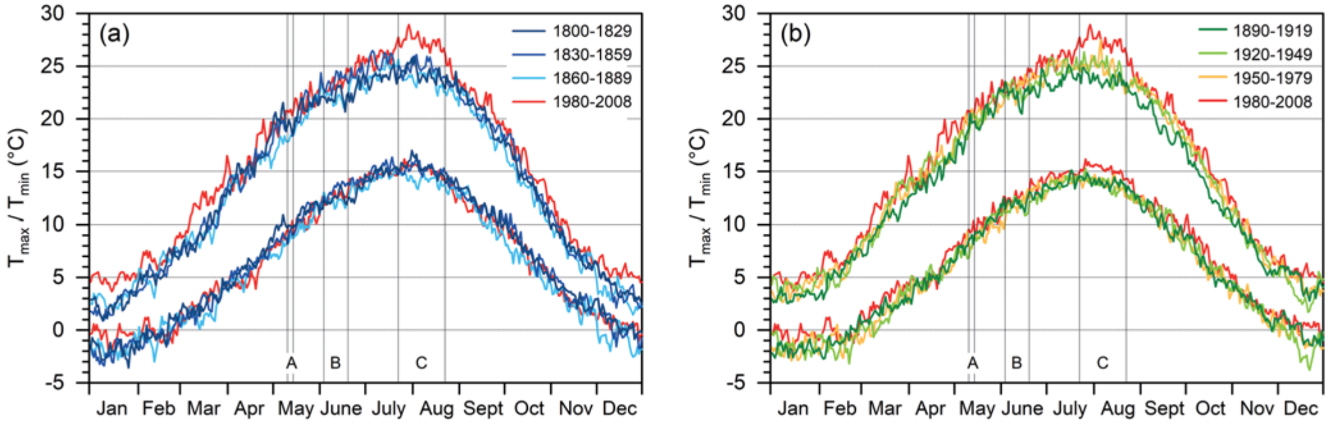

Figure 6: Seasonal cycle of daily minimum and maximum temperatures, *Tmin* and *Tmax* (cf. Section 3.2), for different 30-year time slices (a and b are identical but show different time slices; the most recent period covering only 29 years, 1980–2008, is shown in both subfigure s). The three short periods (A–C) represent well-known singularities of the climate system (A = "Eisheilige", 11–15 May, cold; B = "Schafskälte", 4–20 June, cold; C = "Hundstage", 23 July–23 Aug., hot).

around 1.3 °C before 1980 (e.g., 99th and 95th percentiles, red and blue in Fig. 5c) is larger than that of the lower ones with 0.8 °C (e.g., 1st and 5th percentile). Most striking, again, is the large increase in the values of all percentiles in the second half of the 20th century, which starts somewhat earlier than that of the entire year. The summer median (black curve in Fig. 5c), for example, has increased by 1.3 K from 18.2 °C in the middle of the last century to 19.5 °C for the latest 30-year slice. As already found for the entire year, also in summer the higher percentiles show a larger increase compared to the lower percentiles (e.g., approx. 1.5 K for the 75th and 0.5 K for the 25th percentiles; orange in Fig. 5c). As a consequence, the distribution function has broadened gradually since the beginning of the last century but with the largest increase after the mid-60s (e.g., interquartile range from around 4.5 to 5.5 K; green line in Fig. 5d). In contrast to summer, the winter months show both the largest variability and the largest increase in the values for the lower extreme percentiles (Fig. 5e). The distribution function has become slightly narrower over time, as shown, for example, by the interquartile or the 2σ range (green and blue lines in Fig. 5f) with a negative linear trend of 0.68 and 0.81 K (not shown), respectively, over the entire period shown. Spring and autumn show the smallest changes in the percentiles and the distribution function (not shown).

In conclusion, a general trend toward a broadening of the distribution function in addition to a shift in the mean with a large effect for the tail of the distribution function, which is widely postulated to result from climate change (e.g., IPCC 2012, Fig. 1–2; Hansen and Sato, 2016), is observed in summer but neither in winter nor for the entire year.

5.2 Seasonal cycle

Next, we investigate the seasonal cycles of the daily *Tmin* and *Tmax* (cf. Section 3.2) averaged over 30-year time ranges (except of the last period 1980–2008 with only 29 years because of the end of DWD's observations). Fig. 6 shows that the time slices differ considerably. As already discussed in the previous section, the coldest period regarding *Tmax* is that of 1860–1889, whereas *Tmin* is lowest in the period 1920–1949. As expected, the highest temperature values were recorded during the latest period from 1980 to 2008, but only for *Tmax*. This period had by far the most days in which *Tmax* set a new record. Considerable positive deviations to all other 30-year periods can be observed during the winter (mid-Dec. to mid-Feb.), spring (mainly March and mid-April), and, most conspicuously, from July to mid-August, where the deviation is largest at 3–5 K. By contrast, even though the *Tmin* records in the last time slice are the highest during the 20th century, they are comparable to the periods in the 19th century. The earliest two periods, 1800–1829 and 1830–1859, even had slightly higher *Tmin* values on average compared to 1980–2008.

The variability of the temperature during winter, particularly in December, is also noteworthy. During the periods 1860–1889 and 1920–1949, the lowest December values for *Tmin* and *Tmax* were registered – whereas the remainder of the year does not show other exceptional discrepancies. Singularities of the climate system can be found in some of the periods. The well-known, popularly called Ice Saints (*Eisheilige* in German) between 11 and 15 May (James, 2007), related to frequently occurring cold air outbreaks ("A" in Fig. 6; see Section 5.3 for further details), can hardly be identified in the 30-year means. Only the periods from 1860 to 1889 (light blue line in Fig. 6a) and from 1920 to 1949 (light blue green in Fig. 6b) show a slight, but somehow abrupt decrease in *Tmax* by about 2 K (in the latter period 4 days ahead of the Ice Saints), and a smaller decrease in *Tmin* by about 1 K. This is already an indication that the Ice Saints are a singularity not frequently occurring, which will be studied more in details in Section 5.3c.

The *Schafskälte*, frequently lasting from 4 to 20 June again as a result of cold air outbreaks ("B" in Fig. 6), can be identified in *Tmin* and *Tmax* during all 30-year time slices, except for the second one and the last one. Some of the time slices even exhibit the lowest *Tmax* daily averages from mid-May until mid-September toward the end of the *Schafskälte*. The last singularity, the so-called *Hundstage* (Krüger, 1994) with the core period lasting from 23 July to 23 August, is related to numerous unstable southwesterly weather patterns ("C" in Fig. 6). This less-known singularity is clearly represented in most of the 30-year slices, especially in those two from 1860 to 1919. However, the last period 1980–2008 has the highest *Tmax* values in that time frame.

Most seasonal temperature cycles presented in Fig. 6 show considerable temperature fluctuations in periods of several days to a week (or even longer) – despite the comparatively long averaging time of 30 years, which prevents the characteristic lifetime of cyclones or exceptionally cold or warm years from dominating the statistics. These temperature fluctuations occur during all time slices and seasons and likewise affect *Tmin* and *Tmax*. The variability is highest in the last 30 years and mainly in the summer, which can be related to the broadening of the distribution function in summer as discussed in Section 5.1. During that time slice, most conspicuous are the considerable temperature changes at the beginning and end of April, but also – with a negative sign – at the end of September and in the first 10 days of November. By contrast, the seasonal cycles with respect to *Tmin* are smoothest for the periods 1830–1859 and 1890–1919; with respect to *Tmax*, it is for the period 1950–1979.

5.3 Temperature indices

Climate variability over a long period, including extremes, can be well described by temperature indices. Because of the potential threat to society of days with frost or late frost events in spring, for example, information about their annual number has been collected in some regions since mediaeval times (Zhang et al., 2011). Temperature indices either count the annual number of days exceeding a temperature threshold, accumulate daily temperature differences above or below a defined threshold, or determine the day of the year on which a certain threshold is reached (e.g., Manton et al., 2001; Zhang et al., 2011; Mudelsee, 2020). In our study, we used all three types of temperature indices:

I. Four indices that count the number of days per year above or below a threshold based on *Tmin* and *Tmax* (threshold days, Section 5.3a).

II. Two indices that accumulate differences of *Tmin* or *Tmax* and certain thresholds, and accumulate these differences over an entire year, thus also considering the duration of an event (heat wave and cold spell index; Section 5.3b and 5.3c), and

III. Indices related to a certain day or period in the year where the temperature reaches a certain threshold (late spring frost days and late frost severity index, Section 5.3c).

In the following analyses, years with gaps in the original Karlsruhe temperature series are not considered, even if they were filled with data from other series (cf. Section 3.4) – but depending on the season of these gaps. For example, the year 1944 (gap from 01 Nov) is considered in the quantification of summer/hot days, but not of frost/ice days.

5.3.1 (a) Threshold days

Four threshold days are calculated (e.g., Brown et al., 2010): summer days (SD; $T_{max} \geq 25\,°C$), hot days (HD; $T_{max} \geq 30\,°C$), frost days (FD; $T_{min} < 0\,°C$), and ice days (ID; $T_{max} < 0\,°C$). For the quantification of these threshold days, the continuous temperature values are mapped on dichotomous quantities (0/1). As we do not compare threshold days between different stations, we use predefined, fixed thresholds rather than percentiles. Using fixed thresholds, however, is a very rigid criterion – especially when remembering the uncertainty of approximately 1 K inherent in the construction of *Tmin* and *Tmax* of the new temperature series (see Section 3.2). For example, a day is not classified as a certain threshold day when the observed temperature value is only 0.1 K below or above the defined threshold. To consider the uncertainty in *Tmin* and *Tmax* and to assess the sensitivity of the temperature indices to slight variations in the threshold, we varied the threshold by ±1 K. During the entire period from 1779 to 2008, the average number of hot days (HDs) and summer days (SDs) is 10.5 and 49.6, respectively. Frost days (FDs) and ice days (IDs) were recorded 67.2 and 16.9 times, respectively, on average. Similar to the different percentiles (Fig. 5), most conspicuous in Fig. 7 is the very large increase in HDs and SDs (Figs. 7a and b) toward the end of the series, while FDs and IDs simultaneously decreased (Figs. 7c and d).

A closer examination shows that at the beginning and in the second half of the 19th century (from approximately 1860 to 1920) the number of HDs was lowest with only 10 days on average. In eight years (1805, 1813, 1815/1816, 1829, 1913/1914, 1916), the threshold temperature of 30 °C was not reached even on a single day. Near the middle of the 19th century (ca. 1830–1865) the number of HDs was highest in the entire 100-year period with up to 29 days (1859). The transition to the present warm climate occurred in two major steps, the first from 1920 to 1960 with 1947 being the year with the most HDs until 2003, and the second from the mid-1980s onwards with an even stronger increase. As clearly shown in Fig. 8, lowering or raising the threshold by 1 K has a strong effect on the overall number of HDs. However, the general course of the curve with various warmer- or colder-than-normal intervals essentially remains unchanged.

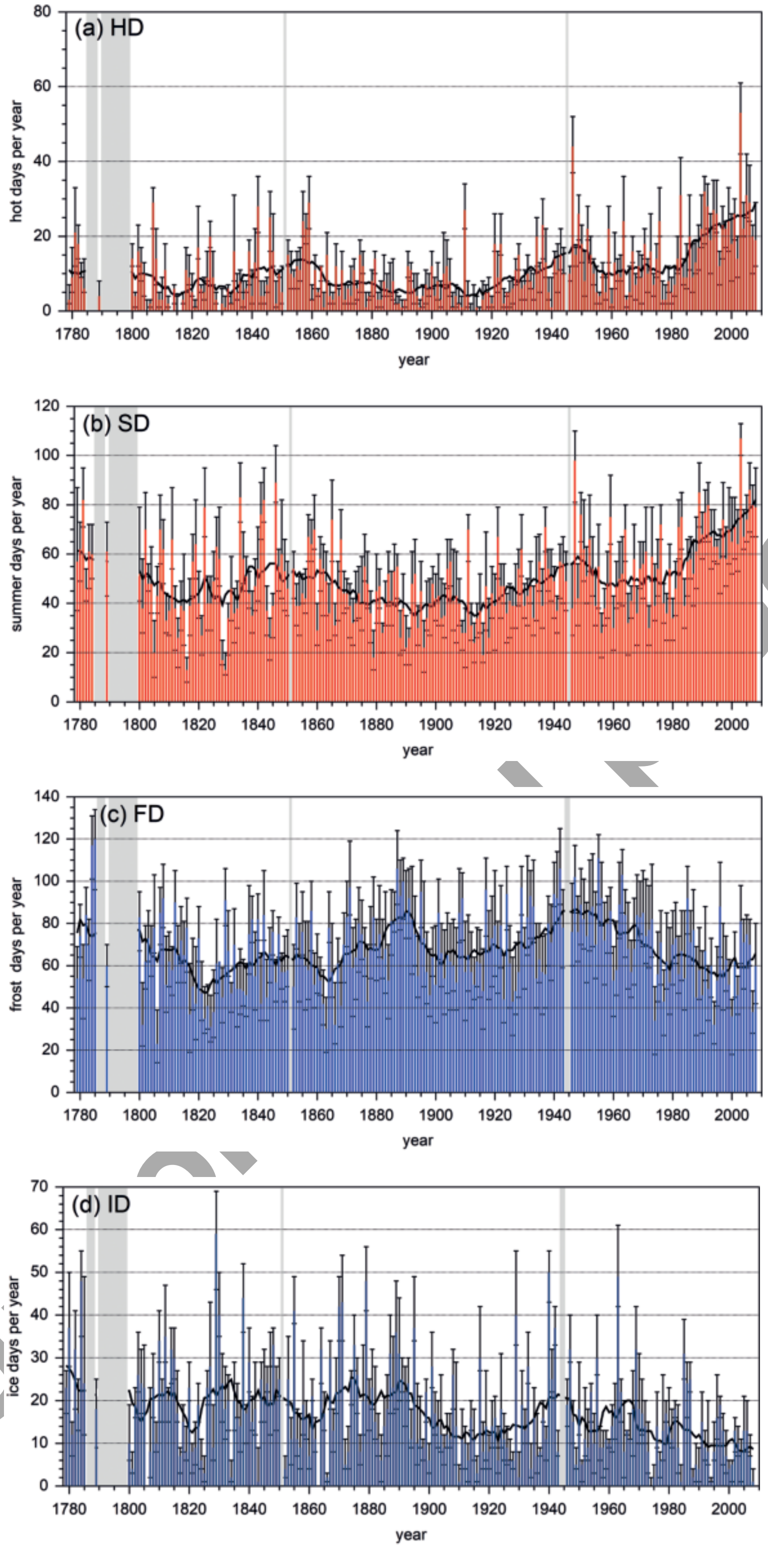

Figure 7: Annual number of (a) hot days (HDs), (b) summer days (SDs), (c) frost days (FDs), and (d) ice days (IDs) between 1779 and 2008 with an 11-year moving average and changing threshold definitions of ±1 °C. Gaps in the original Karlsruhe temperature series are indicated by the grey areas.

Compared to the annual number of HDs, the SDs show a weaker (relative) year-to-year variability, in particular between the second half of the 19th century and the first third of the last century (Fig. 7b). In the former century, the average SD number was 48 without a significant trend. In several years until 1870, more than 60 SDs were recorded. The 19th century, however, also had the coldest summers of the entire record; in particular, the years 1816 (see Section 4.5), 1828 and 1829 had less than 15 SDs, an exceptionally low number. After a

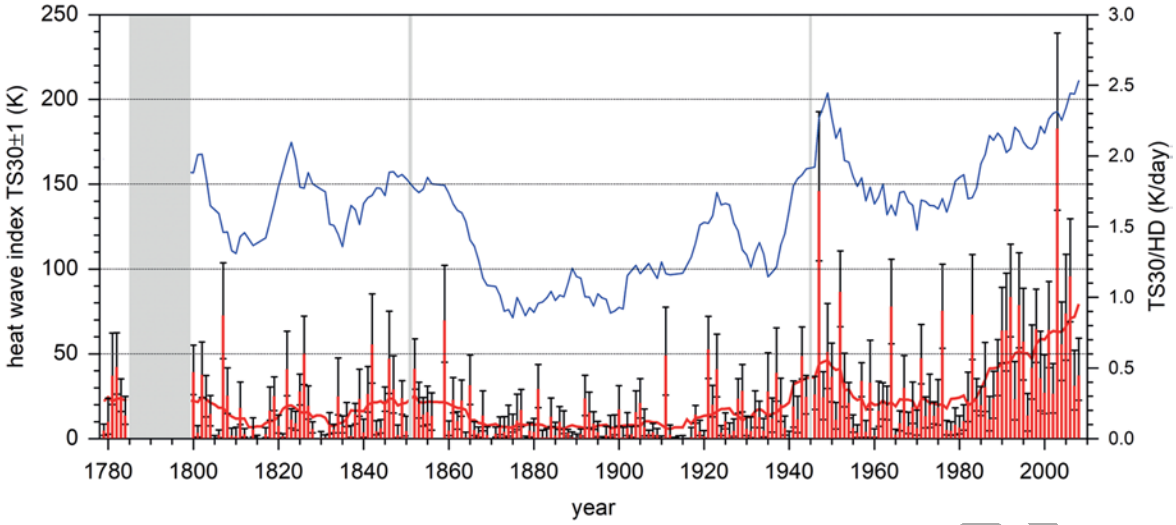

Figure 8: Heat wave index TS30 quantified by the cumulative T_{max} excess above 30 ± 1 °C (red, left axis; cf. Eq. (5.1)) and the 11-year running mean of the ratio TS30/HD (blue, right axis).

slight increase in SDs in the middle of the 19th century, the number was at its lowest from approximately 1870 to 1920. Similar to the HDs, the SDs also increased in two major steps with the strongest increase after 1985. Over the entire record, the ratio of HDs to SDs gradually increased, which can be attributed to the shift of the probability distribution function of *Tmax* as discussed in Section 5.1 (Fig. 5). The time series resulting from a threshold reduced and increased by 1 K are almost parallel to that of the original definition.

The annual number of FDs has two distinct maxima: at the end of the 19th century and near the 1950s (Fig. 7c). These cold periods are framed by several years with a low number of FDs near 1820, 1860, 1900–1940, and, of course, after approximately the 1970s with a gradual decrease until the end of the recording. With a total number of 117 and 120 FDs, respectively, the years of 1784 and 1785 represent the two absolute maxima. Twenty years later in 1806, only 23 such days were registered, being the absolute minimum of the entire series.

The time series of IDs (Fig. 7d) shows a much higher annual variability and a larger uncertainty (error bars) compared to the FDs. Years with a high number of IDs, such as more than 30, are more or less irregularly distributed. The year 1829 has been the coldest year so far with 59 IDs. In addition, two features are obvious: the extended period of a low number of IDs in the first half of the last century, and the strong decrease in recent years. After 1970, only four years have seen more than 20 IDs. During the 19th century, 9 years (≈ 9 %) had less than or equal to 5 IDs, whereas in the 20th century the number slightly increased to 12. *Tmax* did not drop below 0 °C in the years 1806, 1863, and 1974, even when the threshold temperature was reduced 1 K (except for 1974).

When comparing the time series of all four threshold days, similarities and discrepancies can be observed. Although HDs show a larger temporal variability compared to SDs, the two samples are highly correlated ($r = 0.83$, $p < 0.0001$). The same is true for FDs and IDs ($r = 0.60$, $p < 0.0001$). A strong anti-correlation of frost/summer days and, to a lesser degree, of hot/ice days as found in the last 30, could not be observed in times mainly unaffected by climate change. At the beginning of the 19th century, for example, all threshold days are very low in number, whereas between approximately 1910 and 1940, all threshold days show a gradual increase.

(b) Heat Wave Index

Heat waves are one of the primary weather-associated threats to human life in Europe and in Germany (Robinson, 2001; Zacharias et al., 2015). Although heat waves (and cold spells) are not rigorously and universally defined, they are generically considered to be extended periods of unusually high temperature or heat stress. Some authors rely on the duration of a high temperature episode (e.g., more than 3 days above 30 °C) in combination with the mean temperature (e.g., Huth et al., 2000). Important for the physical and physiological effect of heat waves, however, are not only the duration but also the temperature magnitude. Both characteristics are factored into the heat wave index *TS30*, defined as the cumulative *Tmax* excess above 30 °C (Kysel, 2002 and 2010):

$$TS30_y = \sum_{d=1}^{365(366)} (Tmax_y^d - 30\,°C) | Tmax_y > 30\,°C; \quad (5.1)$$

$TS30_y$ is accumulated over all days d within a certain year y that exceed the threshold of 30 °C (again considering an uncertainty range of ±1 K).

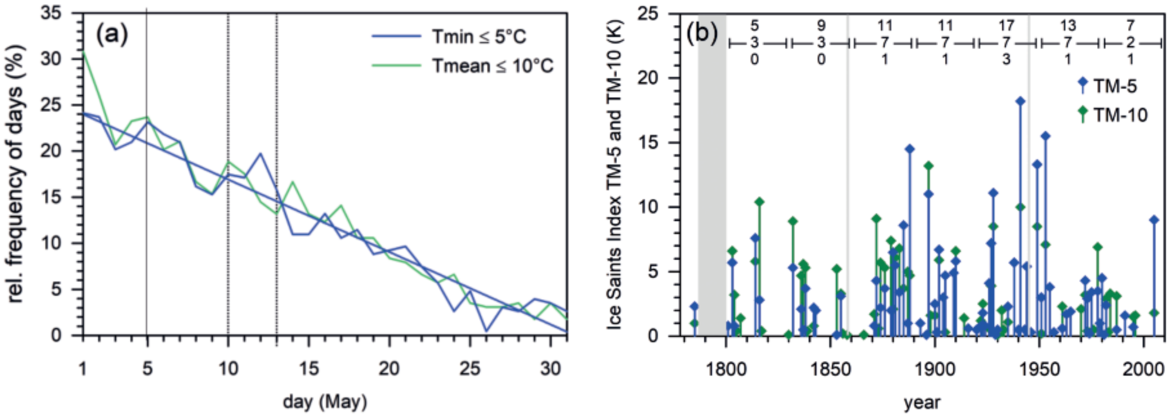

Figure 9: (a) Relative frequency of days with *Tmean* ≤ 10 °C and *Tmin* ≤ 5 °C between 1779 and 2008. (b) Cold spell index for TM-5 (*Tmin*) and TM-10 (*Tmean*) quantified for the 4-day period 10–13 May; the small numbers in the upper part of the diagram indicate the number of Ice Saint events during 30-year slices of all events (top), the 50th (TM-5 ≥ 2.5 K; middle) and 90th (TM-5 ≥ 8.8 K; bottom) percentiles of the TM-5 distribution; grey areas are those intervals with data gaps. The higher the value is, the larger is the temperature deviation from the threshold of *Tmin* = 5 °C.

The time series of *TS30* shown in Fig. 8 is similar to that of HDs (Fig. 7a); in fact, the correlation coefficient $r = 0.93$ ($p \leq 0.00001$) is very high. This result appears at first surprising, because HDs are only counts of the number of days above 30 °C, whereas $TS30_y$ accumulates the excess temperature and, thus, considers the magnitude. However, most of the days counting as HDs are only slightly above the threshold, on average 1.60 ± 0.80 K (= TS30/HD; blue curve in Fig. 8), which also explains the high variability of HDs for changing thresholds (Fig. 7a). In contrast to the number of HDs, *TS30* exhibits a larger annual variability and show a much stronger increase in the past three decades. The latter result is because hot days have become more extreme as a result of the broadening of the distribution function discussed in Section 5.1 (cf. Figs. 5c and d).

Similar to the HDs discussed above, the entire *TS30* series can be roughly divided into four periods. In the first period, from the beginning of the instrumental records to approximately 1870, *TS30* had values between 0 and 72.6 K (mean: 16.6 ± 16.7 K). Afterward, until approximately 1920, heat waves occurred less frequently and/or were less intense (*TS30* between 0 and 49.1 K; mean 7.1 ± 9.1 K). In that time frame, the ratio TS30/HD is the lowest of the entire series; hot days were rare and had a temperature of only ~31 °C on average. In the third period, from approximately 1920 to 1980, *TS30* again shows higher values with a mean of 23.3 ± 25.2 K, i.e., more than three times higher than the period before. Until approximately 1950, *TS30* first increases, with the year 1947 having the highest value at that time (and the highest TS30/HD value), followed again by a decrease. From 1977 to 1981, *TS30* even dropped below 10 K, which means, for example, that only 10 days in the entire year had a *Tmax* of 31 °C, or 5 days of 32 °C. After 1981, and most strongly in recent years, *TS30* increased to the highest values of the entire series on average. In that period with values between 11.4 and 182.8 K (2003), *TS30* is above 30 in almost every year, which has never been the case before. A total of 12 of the 20 strongest heat waves occurred in the last 30 years, five occurred before that in the 20th century and three in the 19th century (1807, 1842, and 1859). The variation of the threshold (i.e., *TS29* or *TS31*) certainly has an effect on the magnitude but does not change the global trend and variability.

(c) Cold spell index

Late spring frosts can potentially cause great damage to agriculture or fruit growing and are therefore very much feared. Particularly before globalization, losses in regional food production caused by frost events often led to famine (Brönnimann, 2015; Adam, 2015). Especially for the second decade of May, examinations have shown that northern weather patterns associated with the influx of Arctic polar air to central Europe are more likely to occur and may lead to late frosts (Tomczyk et al., 2020), such as the Ice Saints. *Ice Saints*. Because of their high relevance to agricultural damage, only frost events in May are considered in the following subsection.

We first determine the thresholds and duration most suitable for detecting cold spells in the Karlsruhe temperature series. Sensitivity studies where we varied the thresholds showed that the two thresholds *Tmin* = 5 °C and *Tmean* = 10 °C are most suitable for the cold spell detection (not shown; note that on days with *Tmin* ≤ 5 °C, ground frost may occur outside of the city). The relative frequency of days with *Tmin* ≤ 5 °C (i.e., the number of days below this threshold normalized by the sum of all days of the series 1800–2008) shows two periods with remarkable and significant positive deviations from the linear trend: between 5 and 7 May and between 10 and 13 May (Fig. 9a). The latter 4-day period represents a slight deviation from the historical definition of the local Ice Saints. The relative frequency of days for the second threshold of

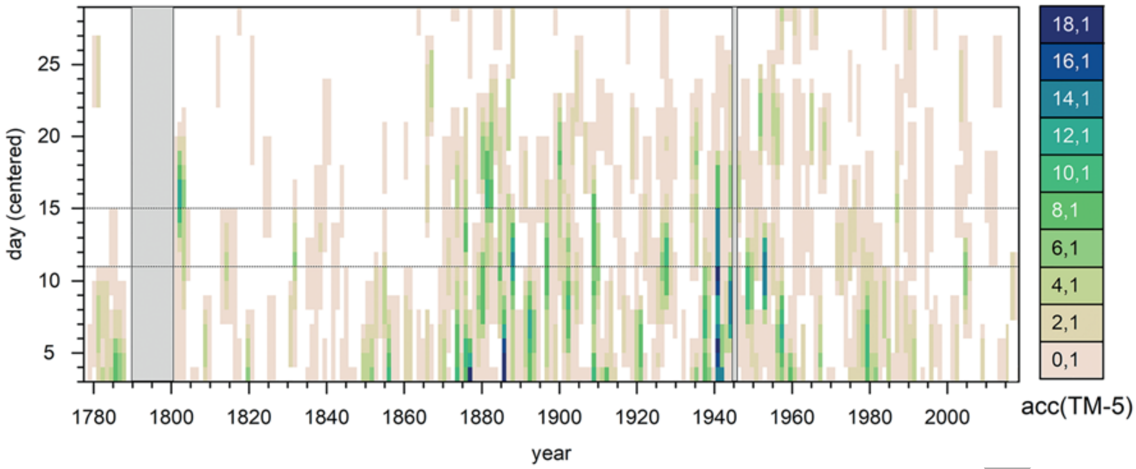

Figure 10: Cold spell index TM-5 accumulated for 5-day periods (displayed as centered differences on the y-axis) between 1800 and 2008 (the horizontal lines indicate the classical Ice Saints period). Each bar indicates the presence of a cold spell lasting over 4 days, whereas the color represents the intensity (TM-5 accumulated over 4-day time frames).

Tmean ≤ 10 °C also shows an increase for these two periods compared to the preceding days, but less significant and lasting one day fewer.

To assess the severity of cold spells, we created two cold spell indices *TM-10* and *TM-5*, which accumulate daily temperature differences to a fixed threshold, similar to the heat wave index *TS30* discussed in the previous subsection. The two indices are quantified from daily *Tmin* and *Tmean* values, respectively, within a 4-day moving window centered around the day of the year *j*:

$$TM\text{-}10_y^j = \sum_{d=1}^{4} (10\,°\mathrm{C} - Tmean_y^d) | Tmean_y^d < 10\,°\mathrm{C} \tag{5.2}$$

$$TM\text{-}5_y^j = \sum_{d=1}^{4} (5\,°\mathrm{C} - Tmin_y^d) | Tmin_y^d < 5\,°\mathrm{C} \tag{5.3}$$

The two cold spell indices, *TM-10* and *TM-5*, are computed not only for the period from 10 to 13 May best representing the Ice Saints as discussed above but also for all days in May.

From 1800 to approximately 1870, the icy saints defined by TM-10 and TM-5 were rare events (Fig. 9b) with intervals of sometimes more than 10 years. Most events show a distinct clustering with 2 to 5 events in short intervals. Not until after 1870 did the Ice Saints emerge as a pronounced singularity of the climate system, affecting most years and with a considerable larger negative temperature anomaly compared to the previous years. Weaker Ice Saints occurred in approximately every second year, whereas extreme Ice Saints (90^{th} percentile of the distribution) occurred most frequently between 1920 and 1949 (see the small numbers in the upper part of Fig. 9b). *TM-5* after 1860 has much larger values compared to *TM-10*, which suggests that the minimum temperature in the night decreased to low values, which was not the case in the preceding years. After approximately 1960, the Ice Saints decreased mainly in intensity, and after 1990, also in frequency. Although climate change is presumably responsible for the low frequency after 1990, this time frame is in some ways similar to the situation before 1860.

Dropping the restriction of cold spells to occur in the window of the Ice Saints, it is found that such events defined by *TS-5* basically can occur throughout the entire month of May; but of course, with a higher frequency and intensity in the first three weeks as a consequence of using a fixed threshold (Fig. 10 shows *TS-5* accumulated over 5-day periods in May).

As discussed above, cold spells in May occurred only infrequently and were not pronounced before 1870. Exceptions to this general behavior are found in the periods 1785–1786, 1801–1802 and in the year 1856. Between 1782 and 1870, no day in May was an FD. The situation changed somewhat abruptly near 1875; from then until approximately 1960, cold spells occurred much more frequently and had considerably lower temperatures than before. Temperatures below the freezing point over the entire 4-day period were even observed in nine years. In addition, significant cold spells now occurred towards the end of May. From 1960 onwards, the number and intensity of cold spells again decreased throughout May. Fig. 10 also highlights that, in some years, cold spells were not singular events, but occurred several times in succession, for example in the years 1874, 1886, 1938, and, most pronouncedly, 1942.

The later an FD occurs in spring, the higher the potential damage to agriculture (Molitor et al., 2014) or trees (Dittmar et al., 2006) because of the advanced growth stage of the plants. As a consequence of natural climate variability, the start of the growing season (SGS) is not constant but depends on the antecedent weather conditions in an individual year. The annual SGS can best be estimated from phenological observations. Because such observations are only infrequently

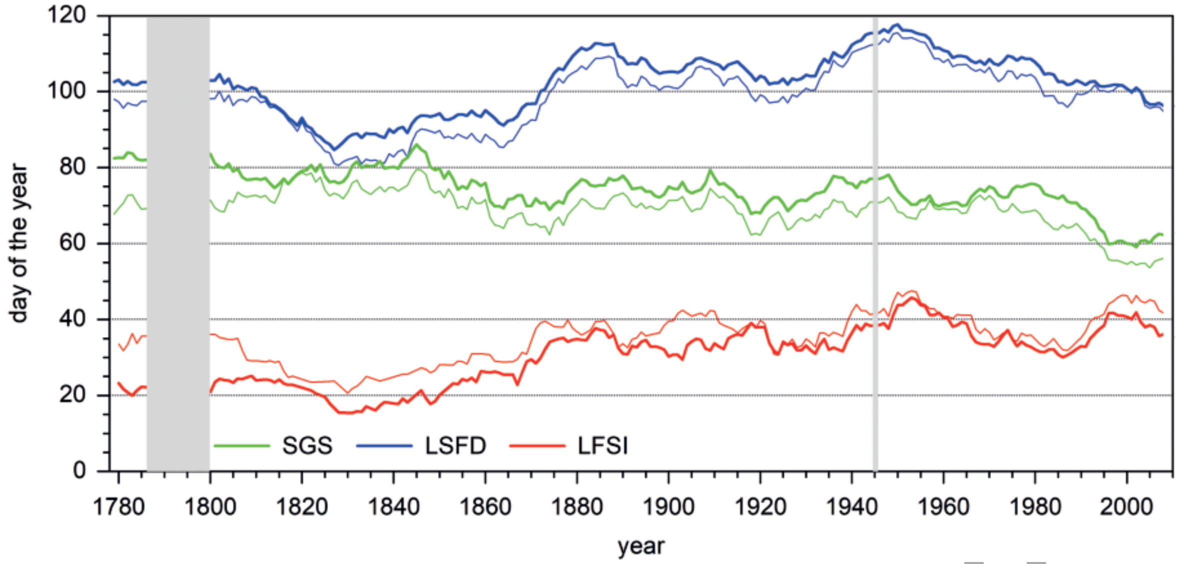

Figure 11: Late frost events: Start of the growing season (SGS), late spring frost days (LSFD) and late frost severity index (LFSI). Thin lines represent the original definition, thick lines are ensemble means based on varying thresholds (see text for further explanation); grey bars indicate a data outage in the first half-year.

available, the SGS can be approximately determined as the day when *Tmin* constantly equals or exceeds a certain threshold. Following Menzel et al. (2003), we define the SGS here as the earliest day in the year where *Tmean* is equal to or above 5 °C on five consecutive days. To consider the sensitivity of the result to slight variations in the threshold, we additionally quantified the mean from different realizations, where the threshold changed from 4.5 to 7.5 °C in increments of 0.5 K (7 realizations). Late spring frost days (LSFD) are defined as the latest day with *Tmin* = 0 °C. Also for LSFD, we varied this threshold from −1 to +2.0 °C, again in increments of 0.5 K. The difference between the two indices defines the late frost severity index LFSI = LSFD − SGS (Mudelsee, 2020). The higher the LFSI value is (in days), the higher the potential threat to the plants will be. In case of a negative differences, i.e., when SGS > LSFD, the LFSI is not defined.

Compared to TM-5 and TM-10, the SGS shows the least temporal variation (Fig. 11). From the beginning of the temperature records until approximately 1860, the values fluctuate around the 80. day of the year (21 March). The other two indices, however, show a reverse behavior: LSFD and LFSI had their minimum in that early period. After 1880, LSFD increased approximately 10–20 days with a maximum near 1950, when frost days occurred even in the last 10 days of May. After that maximum, the values gradually decreased until the end of the temperature record, where no frost day was registered after the beginning of April, representing a shift of 25 days.

The severity index LFSI had the lowest values in the first half of the 19th century, mainly because frost days did not occur after the first week in April. Two maxima can be detected: one near the 1950s due to the very last frost days, and another near the millennium due to a very early start of the growing season. Thus, from the overall course of the LFSI time series, one can conclude that, despite climate change, the risk of frost damage remains at a high level and is almost twice as great compared to that of the first half of the 19th century. In the latter period, the results particularly for SGS and, thus, for LFSI, have their highest sensitivity to variations in the threshold, which is not the case afterwards.

Long-term variability

The change in the annual temperature cycle, particularly in the last 30 years (Fig. 5), inevitably leads to the question of whether the weather has become more extreme in recent years in the sense of a larger variability on scales from days to weeks. The public and the media frequently postulate such an increased temperature variability in spring, presumably resulting from climate change. Whether this perception can be statistically proven is examined using two quantities:

I. the variation coefficient *varcoeff* of *Tmax*, defined as the standard deviation of a sample normalized by its mean, and computed separately for each year and for each month; and

II. the largest increase in *Tmax* between two consecutive 10-day means.

Because the strongest temperature rise is in April and May, following the largest increase in solar insolation, we present here only the results for these two months (Fig. 12a). The parameter *varcoeff* substantially oscillates throughout the entire series and during all months. In April (red curve), a gradual increase in the 11-year moving average is apparent since the beginning of the

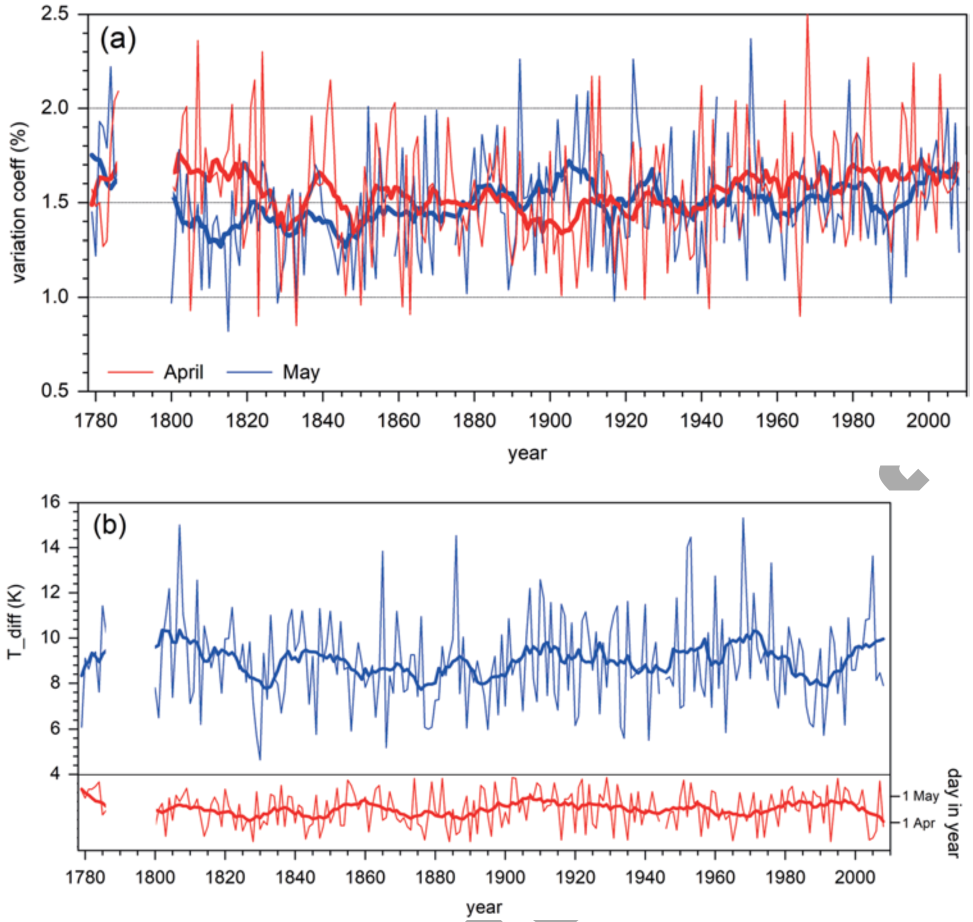

Figure 12: Time series of (a) the variation coefficient of *Tmax* in April and May and (b) the largest temperature changes in the period March to June between two consecutive 10-day periods (top, blue; left y-axis) with the respective day centered between the two periods (bottom, red; right y-axis), including 11-year running means.

last century with a weak, but significant, positive linear trend ($r = 0.27$, $p = 0.002$; not shown). The values of *varcoeff* during the last 30 years, however, are not larger than those of the 30-year period at the beginning of the recording. The month of May (blue curve), by contrast, does not show any trend in the last 100-odd years but increases during the 19th century. More striking, however, is the oscillation of *varcoeff* over periods of 23 years according to a fast Fourier transform (FFT) analysis (not shown). The reason for this periodicity is unclear. Such a periodicity is undetectable in April.

The time series of the largest increase in *Tmax* between two consecutive 10-day means in spring (e.g., the difference between the means 10–19 March and 1–9 March; Fig. 12b) confirm April to be the month with the largest temperature increase of all months (46 % of all cases). However, the annual variability of the *Tmax* difference is large for the magnitude and for the time of the year. According to the power spectrum computed with an FFT (detrended series), the largest variability of T_diff (peak) has a periodicity of 4.1 years, with additional peaks at 2.2 and 3 years (not shown). The time of the year shows the largest peaks at 2.4 and 4.9 years, which is slightly different from those of the magnitude. Large increases of 10 K and more between two consecutive 10-day means occur at irregular intervals, even though some clustering can be detected (e.g., 1804/1807/1812). More importantly, neither the magnitude nor the timing of the largest increase (right axis in Fig. 12b with the center of the period, e.g., 9 March in the above example) show a long-term trend. Only between 1985 and 2008 is a positive trend apparent in the magnitude (0.15 K/year with $r = 0.55$, $p = 0.0018$), which, however, is followed by a decrease until the present. Thus, the statistical analyses cannot confirm the perceived increase in the variability of daily weather.

5.4 The "year without a summer" 1816

Now we return back to the discussion of the year 1816, one of the most unusual years in our recordings. It followed the violent eruption of the Tambora volcano in Indonesia in April 1815, the largest known historic eruption (Oppenheimer, 2003). An equivalent of 50 km^3 of dense rock were estimated to have been expelled into the atmosphere, and huge amounts of sulfur were injected into the stratosphere (Rampino and Self, 1982). Ash particles and sulfate aerosol spread worldwide, and the increased turbidity decreased temperatures in many parts of the world, including cen-

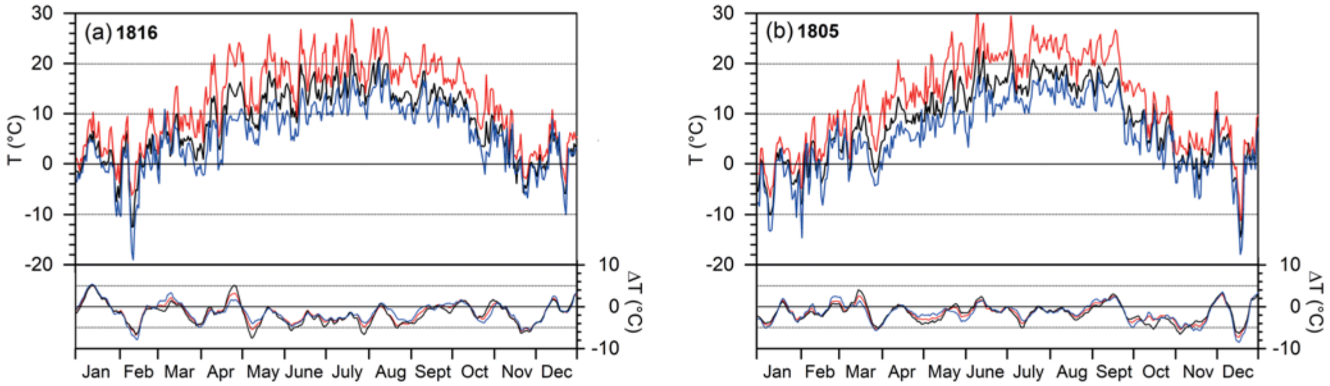

Figure 13: Daily minimum (blue), maximum (red) and mean (black) temperatures (top) and the difference from the 30-year mean for the period 1803–1832 (11-day running means, bottom) for (a) 1816 and (b) 1805.

tral Europe (Brugnara et al., 2015; Brönnimann and Krämer, 2016). The cold and wet conditions in 1816, termed the "year without a summer", led to poor harvests and severe famine, which was responsible for an increase in mortality in central Europe (Luterbacher and Pfister, 2015). Brönnimann (2015) and Brönnimann and Krämer (2016) elaborated on a quite differentiated picture of the effects of Tambora on the weather and climate worldwide, based on a wealth of climate proxy data and observations. They arrived at a decrease of only −0.5 K in the mean global temperature, which can still cause adverse effects. In addition, poor governance was ultimately as important as climate conditions (Brönnimann and Krämer, 2016).

At the Karlsruhe station, the year 1816 with an annual mean of $\overline{T} = 8.24\,°C$ was not the coldest year of the entire temperature record; other years, such as 1805 ($\overline{T} = 8.22\,°C$), 1829 ($\overline{T} = 7.92\,°C$), and 1838 ($\overline{T} = 7.90\,°C$), were slightly colder, but significant famines were not reported. As discussed above, 1816 shows the smallest magnitude of the annual cycle in the monthly means (red box in Fig. 4) and had no single hot day and only 11 summer days, the fewest of the entire record (together with 1839; Fig. 7). In addition, a significant cold spell lasted until 15 May according to *TM-5* (Fig. 10). In the daily values of *Tmin*, *Tmax*, and *Tmean*, the period from mid-March until the end of August, which is most relevant to plant growth and thus to crop yield, was 2.5 K colder (daily mean) compared to the mean of 1803–1832 (Fig. 13a). Temperature anomalies prevailing over several days were up to 5 K; on single days, even up to 10 K. The temperature anomalies mainly affected the higher percentiles of the daily (mean) temperature distribution. Temperature values of the 75th, 90th, or 95th percentiles, for example, were the lowest ever recorded in Karlsruhe (not shown). By contrast, the lower percentiles (e.g., 5th, 10th, 25th) do not show significant deviations from other years. Thus, in 1816, the distribution function of *Tmean* was not entirely shifted to lower values but instead restricted to the side of the higher values, including the tail (note that this change is even more pronounced for *Tmax*). This one-sided anomaly of the distribution function can partly be explained by a higher-than-normal cloud cover at all three observation times of the temperature series. Clouds at the low- or mid-troposphere levels usually have a cooling and warming effect because of reduced insolation and outgoing longwave radiation, respectively. This result can partly explain the reduced seasonal cycle of the temperature in 1816, which is consistent with the analyses at Geneva in Switzerland (Auchmann et al., 2012; Brönnimann, 2015). Other authors have noted that the Tambora eruption occurred at the end of a period of already decreasing temperatures, as documented in the Karlsruhe temperature series, that already started in 1790 as proposed by the Basel time series. The years before 1816/17 were also below average in the number of summer days.

The few summer days in the Karlsruhe temperature series seems to support the hypothesis that changes in atmospheric circulation rather than direct extinction of solar radiation by sulfate aerosol caused the anomalous conditions. An almost summer-long period of approaching Atlantic low pressure systems is consistent with missing summer days and much rain, which farmers complained occurred every day (Brönnimann and Krämer, 2016). Such periods of cyclonic weather conditions, when related to a positive phase of the North Atlantic Oscillation (NAO), typically last several years. From this perspective, the "year without a summer" might have been the consequence of a regional amplification of cyclonicity in Western Europe by indirect Tambora effects. Other unusually cold years, such as 1805, do not show such large deviations from the mean values during summer (Fig. 13b). The year 1805 was unusually cold mainly because of low temperatures down to −20 °C in the winter, which is not really relevant to the agricultural yield.

Only meteorological data at a sub-daily resolution enable us to disentangle what really makes the year 1816 so special, such as the damped diurnal temperature cycle related to cloudiness.

6 Summary and conclusions

Long-term instrumental observations of meteorological parameters are of paramount importance for a better understanding of natural climate variability and the contribution of climate change to the observed changes. A prerequisite, however, is a high temporal resolution of the data, preferably on a daily or even sub-daily basis. The newly digitized Karlsruhe climate series, starting with regular measurements and observations in 1776 (in the archives since mid-1778), is one of the longest series available for Germany. It includes various parameters, such as the temperature, pressure, relative humidity, wind speed and direction, precipitation, cloud cover, and significant weather reports, most of which are reported three times a day. The historical archives from GHCN (Menne et al., 2018) or HISTALP (Auer et al., 2007), for example, only provide the mean monthly temperature.

With great effort, we have digitized the original Karlsruhe climate main series and additional parallel series from handwritten manuscripts archived in the handwritten documents departments of the university libraries of Karlsruhe and Heidelberg, the municipal archive of Mannheim, and the DWD library. All observations have been converted into SI units or contemporary units (e.g., °C, hPa, $m\,s^{-1}$). The temperature time series was additionally homogenized with respect to consistent observation times and referring to an urban boundary site. Furthermore, maximum and minimum temperatures were constructed by applying a mean characteristic daily temperature cycle for 10-day periods.

In this paper, we have analyzed only the Karlsruhe temperature series, mainly for four reasons: Compared to other parameters, such as wind, moisture, and precipitation, the records are mostly complete with only a few gaps; temperature measurements are most reliable; temperature features a characteristic diurnal and seasonal cycle that allows for a simplified homogenization; and temperature best displays the effect of both, natural climate variability on various temporal scales and climate change.

We have performed and discussed several statistical analyses to better understand the effects of climate variability on temperature by extending the daily time series by an additional 84 years (1779–1874 but with a gap of 12 years) out of the 133 years (1878–2008; one year missing) available at that time. The main focus of our study was on the newly processed series prior to 1874 that enables us to better place the dramatic temperature rise and variability in recent years in an extended historical context.

The main new insights we have gained from the first analysis of the long-term Karlsruhe temperature series are the following:

The distribution function of the daily mean temperature shows considerable fluctuations throughout the time series. In the summer months, nearly all percentiles show the strongest variability in the 19th century, while in winter the fluctuations are greatest in the first half of the 20th century. The observed increase especially in the upper tail of the distribution function and thus the broadening of the distribution function over the last decades is unprecedented. The broadening has several consequences, such as a gradual increase in the ratio between hot days and summer days by a factor of four between 1800 and 2008.

When considering only hot or summer days, the period from approximately 1870 to 1920 was the coldest period in the entire record. In that period, the number of hot days is almost half less than before or after. The same applies for the heat wave index. Similar to the percentiles of the upper tail of the distribution function for Tmean, summer days and hot days show an unprecedented increase in the last 30–50 years, whereas, coincidently, frost and ice days have decreased.

The values for *Tmin* for the last 30 years are generally higher than those in the 20th century but very similar to those in the 19th century. The two periods 1800–1829 and 1830–1859 even had slightly higher *Tmin* values on average compared to 1980–2008. The variability is highest in the summer months of the last 30 years, mainly resulting from the broadening of the distribution function.

The entire Karlsruhe temperature series highlights the fact that heat waves, similar to the summer/hot days, were very rare before 1920, being unrepresentative of a period mainly unaffected by climate change. 12 of the 20 strongest heat waves occurred in the last 30 years, including five in the 20th century but also three in the 19th century.

Singularities of the climate system, such as the (cold) *Schafskälte* in June or the (warm) *Hundstage* in July/August, are clearly shown in most periods. The (cold) Ice Saints in May, however, have a high frequency only in the coldest period between 1870 and 1960. They are hardly detectable in the preceding years, due especially to higher *Tmin* (in the period 1800–1870 no single ice day was recorded in May), or in the subsequent years, due mainly to climate change. Also at other stations, such as the DWD station in Munich, Ice Saints in the classical sense cannot be observed (Ehmann, 2020). However, significant Ice Saints, such as in 2005 or 2017, may still occur. Furthermore, cold spells in May are not restricted to the Ice Saint period and could be observed throughout May, especially in the period 1870–1960.

The severity of late spring frosts has gradually increased since around 1830 – with the largest increase between 1830 and 1880 – and remains at a high level. This increase results mainly from later occurrences of frost events, while the start of the growing season has shifted only slightly to earlier days. One can conclude that, despite of climate change, the risk of frost damage remains at a high level and is almost twice as large as for the first half of the 19th century.

The apparent perception that the transition from spring to summer has become shorter with larger temperature changes could not be confirmed by our analyses. Rather, a temperature increase of, for example, more than 10 K between two 10-day periods can be observed in the entire time series (with a somewhat greater accumulation between about 1900 and 1940).

All the above mentioned findings could only be derived from daily or sub-daily temperature values now available for Karlsruhe. We are aware that the Karlsruhe temperature series may still contain errors despite careful processing and multiple testing. Uncertainties also may emerge from the lower standard of measurements in early times compared to the situation today. Therefore, all analyses presented here must be considered with caution. However, the various evaluations do not show any actually implausible outliers or unexplainable discrepancies, which in turn strengthens our confidence in the quality of the data.

In the next step, we envisage statistically evaluating additional climate data, such as precipitation, cloud cover and significant weather observations, both individually and in their context.

Acknowledgements

We thank the mentioned libraries for the possibility of archive research. DWD and NOAA are acknowledged for the provision of data. Map data copyrighted OpenStreetMap contributors and available from https://www.openstreetmap.org. The constructive comments and suggestions of two anonymous reviewer were greatly appreciated and helped to improve the quality of the manuscript.

Appendix

Appendix A: Data

Table A1: Chronology of the observation sites in Karlsruhe of the main climate series (see also Fig. 1).

Period and main observer	Location, barometer elevation	Instruments (thermometer, barometer)
(a) Reconstructed		
1779–1789 J.L. Böckmann	Innerer Zirkel 6, h = 120.4 m asl (location a in Fig. 1)	Mercury barometer with partitions in Paris measure; Reamur-HG-Thermometer
1789–1803 C.W. Böckmann	same location (a)	same instruments
1803–1840 –1821: C.W. Böckmann 1821: L.A. Seeber –1834: G.F. Wucherer –1840: L.A. Seeber	Karlsruher Lyzeum, marketplace, h = 121.1 m (location b)	same instruments; 1808: Fischbein hygrometer after Deluc 1829: August psychrometer
1840–1849	Physikalisches Kabinet, Spitalstrasse, almost same location, but h = 119.4 m (location c)	1942: new instruments from astromonical observ. Univ. Munich; same types
1850–10 Nov 1868 –1855: O. Eisenlohr –1868: A. Heckmann	Lyzeum, marketplace, same location as previous (location d most probably)	
(b) DWD Archive		
1868–24 July 1882	Polytechnicum (TH), Lange Strasse (today: Kaiserstrasse), West wing, h = 123.0 m (location e)	Mercury barometer according to Pfisterer, Bern
1882–07 Mar 1895	relocated within same building, h = 124.4 m (e)	same instruments
Mar 1895–Nov 1898	relocated within same building, h = 121.9 m (e)	1891: renewal of tube of barometer 1895: recording thermometer according to R. Frères, Paris
Dec 1898–30 June 1921	University building, h = 117.5 m (location f in Fig. B2)	1905: station barometer Fuess with reduced scale during operation 1910: additional thermometer shelter mod. Potsdam, with Richard-thermograph 1911: thermograph in shelter
Aug 1921–31 Mar 1937	Durlacher Allee 56, 49° 00′ 29′′ N, 8° 25′ 33′′ E, h = 120.4 m (location g)	Two station barometer, 2 barographs
1 April 1937–31 Oct 1944	Weather station air base, 49° 01′ N, 8° 25′ E, h = 119.7 m (h)	same instruments
1 May 1946–30 Sept 1966	Erzbergerstrasse 35, 49° 01′ 12′′ N, 8° 23′ 24′′ E, h = 115.8 m (i)	
1 Oct 1966–31 Oct 1977	same location, but h = 119.6 m	
1 Nov 1977–31 Oct 2008	Hertzstrasse, 49° 02′ 14′′ N, 8° 21′49′′ E, h = 112.0 m (k)	

Table A2: Sources for the digitization of the Karlsruhe climate series in handwritten (original meteorological diaries, climate tables; a) and printed form (b). Note that most of the partial series have some interruptions. The Manuscript department of the University library (UL) Heidelberg (HD) archives duplicates from the KA originals by O. Eisenlohr including own observations.

Period	Title
(a) Handwritten	
(i) Manuscript department UL KA	
1801–1834	*Carlsruher meteorologische Beobachtungen*
1840–1849	dito
1855–1868	dito
(ii) Manuscript department UL HD	
1778–1789	*Parallelbeobachtungen Eisenlohr Karlsruher Meteorologische Beobachtungen*
1800–1851	dito
1852–1856	dito
(iii) Municipal archive Mannheim	
1852–1856	Deposita of the society for natural history Mannheim, Dr. E. Weber
(iv) DWD Archive, Offenbach/Main	
1852–1854	ARCHIV-OF-FILM (duplicate from originals by R. Fecht, Mannheim, 1934)
1868–1875	ARCHIV-OF-FILM (Climate tables weather station Karlsruhe)
1937–1944	Climate station University Karlsruhe
1937–1945	Climate station Airport Karlsruhe
(b) Print	
1804–	*Karlsruher Zeitung*: Regularly extracts from the met. Journals
1840–	*Karlsruher Zeitung*: Daily reports
1850–1868	*Carlsruher Tageblatt*: Daily observations from private station at the botanic garden

Table A3: Major gaps of the Karlsruhe temperature series between 1779 and 2008. The indices (a–d) mark other data series used to close some of the gaps (a = parallel observation by Klauprecht, adjusted to the location; b = parallel observation by Weber, no adjustment; c = main series Mannheim, adjusted to the location; d = DWD station Rheinstetten WMO code 10731, no adjustment).

time period	days
01 Jan 1787–31 Dec 1788	731
01 Jan 1790–31 Dec 1799	3652
07 Aug 1851–30 Nov 1851	116[a]
01–10 Jan 1855	10[b]
11–20 Aug 1857	10[c]
11–20 May 1858	10[c]
17–18 + 21 July 1870;	2+1[c]
01 Nov 1944–30 Sept 1945	334
01 Nov–31 Dec 2008	61[d]

Appendix B: Figures

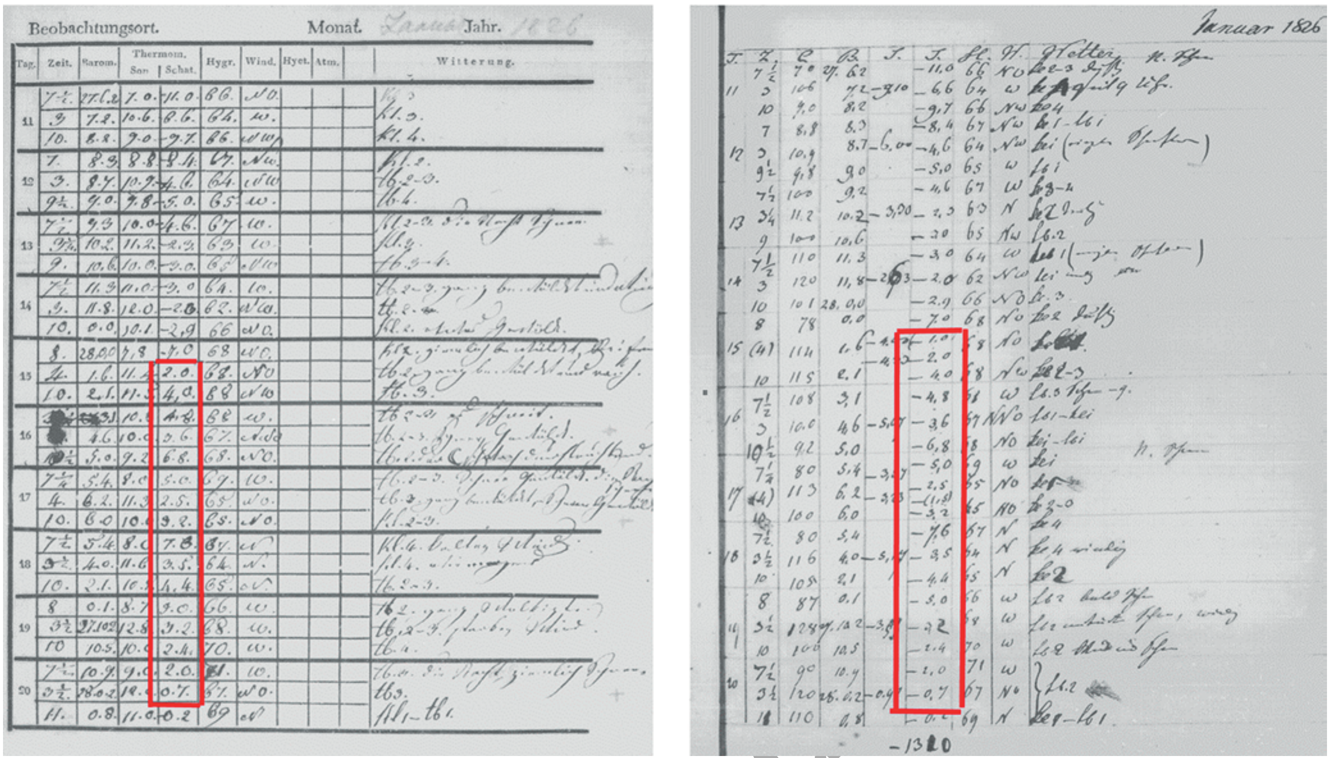

Figure B1: Example of handwritten climate series from the manuscript departments of the university library Karlsruhe (Handschriftenabteilung UL KA, HS 101 – Ed. 1826; left) and Heidelberg (UL HD, HS 381: 1825–1826; right) observation journals for the 2nd decade of Jan 1826. Red framed is the observed temperature between 15 and 20 Jan. 1826 with different signs.

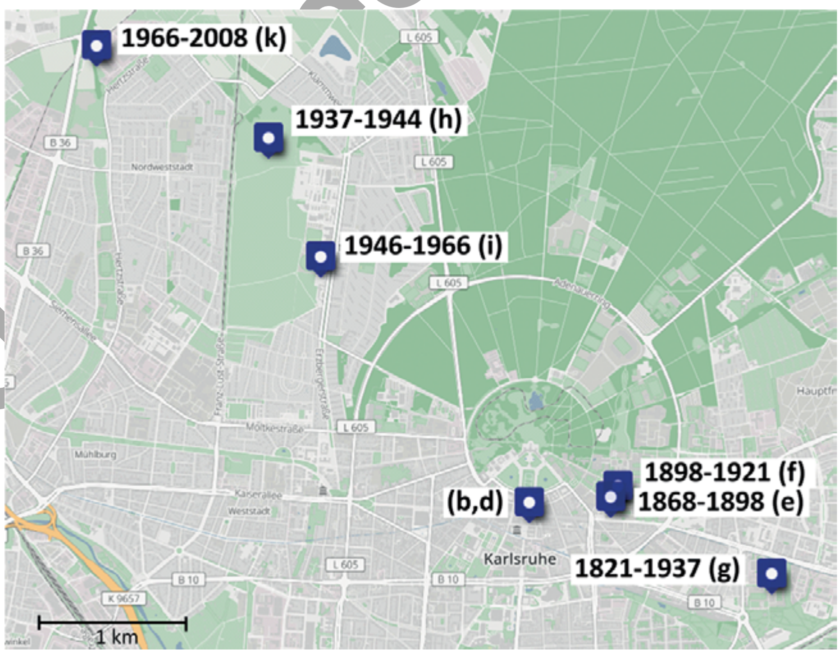

Figure B2: Meteorological observation sites after 1868 (b, d refer to the site shown in Fig. 1); Map from OpenStreetMap data, produced via http://umap.openstreetmap.fr.

References

Adam, T., 2015: Feuer, Fluten, Hagelwetter: Naturkatastrophen in Baden-Württemberg. – Konrad Theiss Verlag, Stuttgart, Germany. 224 pp.

Ansell, T.J., P.D. Jones, R.J. Allan, D. Lister, D.E. Parker, M. Brunet, A. Moberg, J. Jacobeit, P. Brohan, N. Rayner, and others, 2006: Daily mean sea level pressure reconstructions for the European–North Atlantic region for the period 1850–2003. – J. Climate **19**, 2717–2742, DOI:10.1175/JCLI3775.1.

Aspaas, P.P., T.L. Hansen, 2012: The Role of the Societas Meteorologica Palatina (1781–1792) in the History of Auroral Research. – Acta Borealia **29**, 157–176, DOI:10.1080/08003831.2012.732283.

Auchmann, R., S. Brönnimann, L. Breda, M. Bühler, R. Spadin, A. Stickler, 2012: Extreme climate, not extreme weather: the summer of 1816 in Geneva, Switzerland. – Climate Past **8**, 325–335. DOI:10.5194/cp-8-325-2012.

Auer, I., R. Böhm, A. Jurkovic, W. Lipa, A. Orlik, R. Potzmann, W. Schöner, M. Ungersböck, C. Matulla, K. Briffa, and others, 2007: HISTALP—historical instrumental climatological surface time series of the Greater Alpine Region. – Int. J. Climatol. **27**, 17–46. DOI:10.1002/joc.1377.

Böhm, R., 2006: Homogenisierung langer Klimareihen des Hohenpeißenbergs und des Alpenraums. – GAW Brief des Deutschen Wetterdienstes, Meteorologisches Observatorium Hohenpeißenberg, No 36.

Brown, P.J., R.S. Bradley, F.T. Keiming, 2010: Changes in Extreme Climate Indices for the Northeastern United States, 1870–2005. – J. Climate **23**, 6555–6572.

Brönnimann, S., 2015: Climatic Changes since 1700. – Advances in Global Change Research No. 55, Springer, Switzerland, 360 pp.

Brönnimann, S., D. Krämer, 2016: Tambora and the “Year Without a Summer” of 1816. A Perspective on Earth and Human Systems Science. – Geographica Bernensia G90, 48 pp. DOI:10.4480/GB2016.G90.01.

Brugnara, Y., R. Auchmann, S. Brönnimann, R.J. Allan, I. Auer, M. Barriendos, H. Bergström, J. Bhend, R. Brazdil, G.P. Compo, R.C. Cornes, F. Dominguez-Castro, Van A.F.V. Engelen, J. Filipiak, J. Holopainen, M. Kunz, J. Luterbacher, M. Maugeri, L. Mercalli, A. Moberg, C.J. Mock, G. Pichard, L. Reznicova, G. Van Der Schrier, V. Slonosky, Z. Ustrnul, M.A. Valente, P. Winkler, A. Wypych, X. Yin, 2015: A collection of sub-daily pressure and temperature observations for the early instrumental period with a focus on the year without a summer 1816. – Climate Past, **11**, 1027–1047, DOI:10.5194/cp-11-1027-2015.

Brunner, B., 2009: Nach Amerika: die Geschichte der deutschen Auswanderung. – C.H. Beck, Beck’sche Reihe, 252 pp.

Compo, G.P., J.S. Whitaker, P.D. Sardeshmukh, N. Matsui, R.J. Allan, X. Yin, B.E. Gleason, R. Vose, G. Rutledge, P. Bessemoulin and others, 2011: The twentieth century reanalysis project. – Quart. J. Roy. Meteor. Soc. **137**, 1–28, DOI:10.1002/qj.776.

Cubasch, U., C. Kadow, 2011: Global climate change and aspects of regional climate change in the Berlin-Brandenburg region. – Die Erde **142**, 3–20.

Dittmar, C., W. Fricke, W. Elling, 2006: Impact of late frost events on radial growth of common beech (Fagus sylvatica L.) in Southern Germany. – Eur. J. Forest Res. **125**, 249–259, DOI:10.1007/s10342-005-0098-y.

DWD, 2020: Climate Data Center (CDC). – ftp://opendata.dwd.de/climate_environment/CDC; accessed 20 August 2020.

DWD, 2021a: Temperatur: vieljährige Mittelwerte 198–2010. – https://www.dwd.de/DE/leistungen/klimadatendeutschland/mittelwerte/temp_8110_fest_html.html%3Fview%3DnasPublication; accessed 25 Nov 2021.

DWD, 2021b: Open Data Server. – https://opendata.dwd.de/climate_environment/CDC/observations_germany/climate/daily/kl/historical/, accessed 25 Nov 2021.

Ehmann, Ch., 2020: Analysis of the DWD station Munich city (ID 03379). – Personal communication.

Faist, T., J. Schade, 2013: The Climate-Migration Nexus: A reorientation. – Springer, Dordrecht, The Netherlands, 259 pp., DOI:10.1007/978-94-007-6208-4.

Glaser, R., I. Himmelsbach, A. Bösmeier, 2017: Climate of migration? How climate triggered migration from southwest Germany to North America during the 19th century. – Climate Past, **13**, 1573–1592.

Hansen, J., M. Sato, 2016: Regional climate change and national responsibilities. – Env. Res. Lett. **11**, 34009, DOI:10.1088/1748-9326/11/3/034009.

Heinemann, H., 1994: Homogenisierung der Säkularreihe der Jahresmitteltemperaturen in Bremen. – Meteorol. Z. **3**, 35–38.

Höschele, K., M. Kalb, 1988: Das Klima ausgewählter Orte der Bundesrepublik Deutschland: Karlsruhe. – Berichte des Deutschen Wetterdienstes No. 174, 228 pp.

Huth, R., J. Kysel, L. Pokorná, 2000: A GCM simulation of heat waves, dry spells, and their relationships to circulation. – Climate Change, **46**, 29–60.

IPCC, 2012: Managing the Risks of Extreme Events and Disasters to Advance Climate Change Adaptation. A Special Report of Working Groups I and II of the Intergovernmental Panel on Climate Change [Field, C.B., V. Barros, T.F. Stocker, D. Qin, D.J. Dokken, K.L. Ebi, M.D. Mastrandrea, K.J. Mach, G. -K. Plattner, S.K. Allen, M. Tignor, P.M. Midgley (Eds.)]. – Cambridge Univ Press, Cambridge, United Kingdom and New York, NY, USA, 582 pp.

James, P., 2007: An objective classification method for Hess and Brezowsky Grosswetterlagen over Europe. – Theor. Appl. Climatol. **88**, 17–42, DOI:10.1007/s00704-006-0239-3.

Kämtz, L.F., 1831: Lehrbuch der Meteorologie. – Gebauerschen Buchhandlung,102 pp.

Kaspar, F., L. Hannak, K.-J. Schreiber, 2016: Climate reference stations in Germany: Status, parallel measurements and homogeneity of temperature time series. – Adv. Sci. Res. **13**, 163–171, DOI:10.5194/asr-13-163-2016.

Krüger, L., 1994: Wiederkehrende Witterungen. – In: Wetter und Klima. – Springer, Berlin, Heidelberg, DOI:10.1007/978-3-642-78927-4_22.

Kütting, H., M.J. Sauer, 2011: Elementare Stochastik. – Spektrum Akademischer Verlag, 414 pp.

Kysel, J., 2002: Temporal fluctuations in heat waves at Prague–Klementinum, the Czech Republic, from 1901–97, and their relationships to atmospheric circulation. – Int. J. Climatol. **22**, 33–50.

Kysel, J., 2010: Recent severe heat waves in central Europe: how to view them in a long-term prospect? – Int. J. Climatol. **30**, 89–109.

Luterbacher, J., C. Pfister, 2015: The year without a summer. – Nature Geosci. **8**, 246–248, DOI:10.1038/ngeo2404.

Manton, M.J., P.M. Della-Marta, M.R. Haylock, K. Hennessy, N. Nicholls, L. Chambers, D. Collins, G. Daw, A. Finet, D. Gunawan, and others, 2001: Trends in extreme daily rainfall and temperature in Southeast Asia and the South Pacific: 1961–1998. – Int. J. Climatol. **21**, 269–284. DOI:10.1002/joc.610.

McLeman, R.A., 2011: Settlement abandonment in the context of global environmental change. – Glob. Env. Change **21**, 108–120, DOI:10.1016/j.gloenvcha.2011.08.004.

Menne, M.J., C.N. Williams, 2009: Homogenization of Temperature Series via Pairwise Comparisons. – J. Climate. **22**, 1700–1717, DOI:10.1175/2008JCLI2263.1.

Menne, M.J., C.N. Williams, B.E. Gleason, J.J. Rennie, J.H. Lawrimore, 2018: The Global Historical Climatology Network Monthly Temperature Dataset, Version 4. – J. Climate **31**, 9835–9854, DOI:10.1175/JCLI-D-18-0094.1.

Menzel, A., G. Jakobi, R. Ahas, H. Scheifinger, N. Estrella, 2003. Variations of the climatological growing season (1951–2000) in Germany compared with other countries. – Int. J. Climatol. **23**, 793–812, DOI:10.1002/joc.915.

Mestre, O., C. Gruber, C. Prieur, H. Caussinus, S. Jourdain, 2011: SPLIDHOM: A Method for Homogenization of Daily Temperature Observations. – J. Appl. Meteor. Climatol. **50**, 2343–2358, DOI:10.1175/2011JAMC2641.1.

Molitor, D., A. Caffarra, P. Sinigoj, I. Pertot, L. Hoffmann, J. Junk, 2014: Late frost damage risk for viticulture under future climate conditions: a case study for the Luxembourgish winegrowing region. – Austral. J. Grape Wine Res. **20**, 160–168, DOI:10.1111/ajgw.12059.

Mudelsee, M., 2020: Statistical Analysis of Climate Extremes. – Cambridge Univ. Press, Cambridge, U.K., 200 pp.

Olbers, D., 2013: The temperature in Bremen since 1803–embedding data fragments into homogeneous time series. – Meteorol. Z. **22**, 75–88. DOI:10.1127/0941-2948/2013/0404.

Oppenheimer, C., 2003: Climatic, environmental and human consequences of the largest known historic eruption: Tambora volcano (Indonesia) 1815. – Prog. Phys. Geogr. Earth Env. **27**, 230–259, DOI:10.1191/0309133303pp379ra.

Peterson, T.C., D.R. Easterling, T.R. Karl, P. Groisman, N. Nicholls, N. Plummer, S. Torok, I. Auer, R. Boehm, D. Gullett, L. Vincent, R. Heino, H. Tuomenvirta, O. Mestre, T. Szentimrey, J. Salinger, E.J. Førland, I. Hanssen-Bauer, H. Alexandersson, P. Jones, D. Parker, 1998: Homogeneity adjustments of in situ atmospheric climate data: A review. – Int. J. Climatol. **18**, 1493–1517, DOI:10.1002/(SICI)1097-0088(19981115)18:13<1493::AID-JOC329>3.0.CO;2-T.

Rampino, M.R., S. Self, 1982: Historic eruptions of Tambora (1815), Krakatau (1883), and Agung (1963), their stratospheric aerosols, and climatic impact. – Quart. Res. **18**, 127–143. DOI:10.1016/0033-5894(82)90065-5.

REKLIP, 1995: Klimaatlas Oberrhein Mitte-Süd. – Trinationale Arbeitsgemeinschaft Regio-Klima-Projekt, REKLIP, 157 pp., https://reklip.org.

Robinson, P.J., 2001: On the definition of a heat wave. – J. Appl. Meteor. **40**, 762–775, DOI:10.1175/1520-0450(2001)040<0762:OTDOAH>2.0.CO;2.

Schnelle, F., 1955: Pflanzenphänologie. – Akad. Verlagsges., Geest and Portig KG, Leipzig, Germany, 298 pp.

Trigo, R.M., R. García-Herrera, J. Díaz, I.F. Trigo, M.A. Valente, 2005: How exceptional was the early August 2003 heatwave in France? – Geophys. Res. Lett. **32**, L10701, DOI: 10.1029/2005GL022410.

Tomczyk, A.M., K. Szyga-Pluta, E. Bednorz, 2020: Occurrence and synoptic background of strong and very strong frost in spring and autumn in Central Europe. – Int. J. Biometeorol. **64**, 59–70, DOI:10.1007/s00484-019-01793-z.

Vose, R.S., R.L. Schmoyer, P.M. Steurer, T.C. Peterson, R. Heim, T.R. Karl, J. Eischeid, 1992: The Global Historical Climatology Network: Long-term monthly temperature, precipitation, sea level pressure, and station pressure data. – Carbon Dioxide Information Analysis Center, Tech. Rep. ORNL/CDIAC-53, 325 pp., DOI:10.2172/10178730.

Winkler, P., 2009: Revision and necessary correction of the long-term temperature series of Hohenpeissenberg, 1781–2006. – Theor. Appl. Climatol. **98**, 259–268, DOI: 10.1007/s00704-009-0108-y.

Wulfmeyer, V., I. Henning-Müller, 2006: The climate station of the University of Hohenheim: analyses of air temperature and precipitation time series since 1878. – Int. J. Climatol. **26**, 113–138, DOI:10.1002/joc.1240.

Zacharias, S., C. Koppe, H.-G. Mücke, 2015: Climate change effects on heat waves and future heat wave-associated IHD mortality in Germany. – Climate **3**, 100–117.

Zhang, X., L. Alexander, G.C. Hegerl, P. Jones, A.K. Tank, T.C. Peterson, B. Trewin, F.W. Zwiers, 2011: Indices for monitoring changes in extremes based on daily temperature and precipitation data. – Climate Change **2**, 851–870, DOI: 10.1002/wcc.147.